Supplement

Section 2.1 states "The effect of this update results in our model being able to fit the historical climate record with higher values of climate feedback, especially for strong aerosol cooling (see Fig S1 and supplement for more information)". Figure S1 illustrates the impact of updating Eq. (2) in our model to be comparable to the formulation in Bony et al. (2006) and Schwartz (2012). This figure displays the change in GMST anomaly in 2100 relative to pre-industrial (ΔT_{2100}) as a function of λ_{Σ} and AER RF_{2011} for the two formulations of Eq. (2). Figure S1a uses the previous version of the EM-GC, where Q_{OCEAN} was subtracted outside of the climate feedback multiplicative term, and Fig. 1b uses the new version of the EM-GC where Q_{OCEAN} is subtracted within the climate feedback multiplicative term.

In the EM-GC framework, we calculate our value of Q_{OCEAN} by finding the κ needed to multiply the temperature difference between the atmosphere and the ocean to fit the observed OHC record. The model iterates over the ocean module, specifically the value of $\Delta T_{OCEAN,HUMAN}$ in Eq. (4), until the EM-GC converges on an estimate of κ for a single OHC record and value of AER RF_{2011}. Figure S1 illustrates that the effect of changing Eq. (2) in the EM-GC impacts our estimates of the rise in ΔT_{2100} at high values of AER RF_{2011}. Strong aerosol cooling results in the ocean taking up more heat from the atmosphere than in the previous version of the EM-GC. The larger value of Q_{OCEAN} results in a higher value of climate feedback needed to fit the historical climate record, because both AER RF_{2011} and Q_{OCEAN} are acting to cool the climate system. The higher values of climate feedback increase our maximum value of ΔT_{2100}. This change brings some of the projections of ΔT_{2100} from the EM-GC closer to values of ΔT_{2100} from the CMIP6 multi-model ensemble.

Section 2.2.3 states "Figure S2 shows the ozone RF time series used in this analysis and the supplement provides more information about the creation of the time series for the RF due to O_3^{TROP}". Figure S2 displays the time series of tropospheric ozone RF used in our analysis for the various SSPs. Tropospheric ozone is an important GHG that rivals nitrous oxide as the third most important anthropogenic GHG. We include the RF due to tropospheric ozone (O_3^{TROP}) in our model for completion, even though the SSP database does not provide RF estimates for the various SSPs. We use values from the RCP scenarios provided by the Potsdam Institute for Climate Impact Research (Meinshausen et al., 2011). The values of the RF due to O_3^{TROP} for SSP1-1.9 and SSP1-2.6 are from the RCP2.6 pathway. The RCP4.5 time series of O_3^{TROP} is used for SSP2-4.5, the RCP6.0 time series is used for SSP4-6.0, and the RCP8.5 time series is used for SSP5-8.5. We create linear combinations of RCP2.6 and RCP8.5 to generate two new time series of the RF due to O_3^{TROP} for SSP4-3.4 and SSP3-7.0. There is a large gap between the time series of the RF due to O_3^{TROP} for RCP6.0 (shown as SSP4-6.0) and RCP8.5 (shown as SSP5-8.5) in Fig. S2. We created a time series that would split the difference between the two RCPs to represent the RF due to O_3^{TROP} for SSP3-7.0. The SSP4-3.4 time series of the RF due to O_3^{TROP} that was created lies in between the RCP2.6 (shown as SSP1-2.6) and RCP4.5 (shown as SSP2-4.5) time series in Fig. S2.

Section 2.2.8 states “Figure S4 shows the five OHC records as well as the multi-measurement average”. Figure S4 displays the five OHC content data sets, as well as the multi-measurement average, plotted as a function of time and normalized to year 1986. This figure illustrates how the shapes of the different OHC records compare. Each of the time series represents the amount of heat stored in the top 700 m of the world’s oceans for that specific data set. Carton et al. (2018) is the shortest data set, and only spans 36 years (1982-2017). The second shortest record is Balmaseda et al. (2013a), which spans 52 years (1958.5-2009.5). Ishii et al. (2017) is the record in the middle with a range of 63 years (1955-2017). Both Cheng et al. (2017) and Levitus et al. (2012) have records that span 65 years (1955-2019). The length of the data set and the shape of the curve affect the estimate of ocean heat export (OHE), because we calculate OHE by taking a linear fit to the full OHC time series. Balmaseda et al. (2013a) has the lowest estimate of OHE because the slope of the curve is relatively shallow, due to the fact that it slightly rises, then decreases at the start of the record. Carton et al. (2018) has the highest estimate of OHE because the slope of the curve is the steepest of the five records.

Section 2.2.8 also says “For these five OHC data sets, uncertainty estimates are not always provided. Furthermore, some studies that do provide uncertainties give estimates that seem unreasonably small (see Fig S5 and supplement)” and “Figure S5 and the supplement provide more detail on the creation of this time dependent uncertainty estimate for OHC”. Figure S5 shows the multi-measurement average as well as the five OHC data records as a function of time, the uncertainty for each corresponding data set, and the combined uncertainty used in this analysis. Panel (a) shows the multi-measurement OHC average with the standard deviation of the mean plotted around the average time series. The standard deviation is large at the beginning of the time series, due to the spread in the estimates of OHC between the different records (illustrated in Fig. S4). The standard deviation decreases as the various OHC records converge near a similar estimate. The standard deviation is zero in 1986 because we normalized all of the time series to zero in this year to create the multi-measurement average. Because of this normalization, the standard deviation of the mean is not a realistic measure of uncertainty for the five OHC time series.

Panels (b), (c), (d), (e), and (f) display the uncertainty estimates for the five OHC data records. We use the standard deviation of the mean of five ensemble members of the European Centre for Medium-Range Weather Forecasts Ocean ReAnalysis System 4 (ORSA) (Balmaseda et al., 2013b) for the Balmaseda et al. (2013a) record. The standard deviation is plotted in panel (b) as the dotted blue line. The standard deviation is small at the beginning of the record, because the five ensemble members started at similar values of OHC in 1958 and diverged over time. The combined uncertainty of the standard deviation of the mean and the Cheng et al. (2017) estimate is plotted as a dashed blue line. Panel (c) shows the Levitus et al. (2012) time series for the top 700 m updated to the end of 2019. The Levitus time series utilizes the standard error over the whole ocean for their uncertainty estimate and is plotted as the dotted light blue line. The standard error is a very small uncertainty estimate compared to the other OHC data records, which is unreasonable considering the large variations in OHC between the different records. We use the standard deviation of eight reanalysis experiments to represent the uncertainty associated with the Carton et al. (2018) OHC record and is plotted as a dotted orange line in panel (e). The standard deviation of the mean is rather small, which also is unrealistic. Panel (f) displays the Cheng et al. (2017) OHC record updated through the end of 2019 with the 1σ uncertainty. This uncertainty does not vary much throughout the data record, making it more realistic as an estimate for such an uncertain quantity as OHC. We created the combined uncertainty estimate of the standard deviation of the mean and the Cheng et al. (2017) 1σ uncertainty to have the largest uncertainty possible due to the fact that OHC varies between the different records. The EM-GC cannot achieve $\chi^2_{\mathrm{OCEAN}} \leq 2$ for Balmaseda et al. (2013a), Levitus et al (2012), and Carton et al. (2018) using their own respective estimates of uncertainty. Creating one uncertainty estimate to be used for all of the OHC records provides consistency and allows the EM-GC to achieve good fits between the observed and modeled OHC.

Section 2.5 states "See Fig. S7 for unweighted ECS values and Section 3.2 states "See Fig S7 for results without aerosol weighting". Figure S7 displays the values of ECS using the EM-GC and the CMIP6 multi-model ensemble. The EM-GC box contains the 25$^{\mathrm{th}}$, 50$^{\mathrm{th}}$, and 75$^{\mathrm{th}}$ percentiles, the whiskers denote the 5$^{\mathrm{th}}$ and 95$^{\mathrm{th}}$ percentiles, and the stars represent the minimum and maximum values of ECS. The box labeled CMIP6 is unchanged from Fig. 7. The values of ECS are not treated with the aerosol weighting described in Sect. 2.5. This figure shows that most of the estimates of ECS found using the EM-GC are concentrated towards small values of ECS, due to the fact that the majority of the EM-GC model runs with good fits to the climate record (χ^2_{ATM}, χ^2_{RECENT}, and χ^2_{OCEAN}) have weak aerosol cooling and low values of λ_{Σ} (Fig. 5b). We use the aerosol weighting method to assign the same weights for the IPCC 2013 "likely" range limits of AER RF_{2011} of −0.4 and −1.5 W m^{-2} at the one sigma values of a Gaussian, and the −0.1 and −1.9 W m^{-2} are at the two sigma values of a Gaussian. Using the aerosol weighting method adjusts our estimates of ECS so that the calculated percentiles occur at higher values.

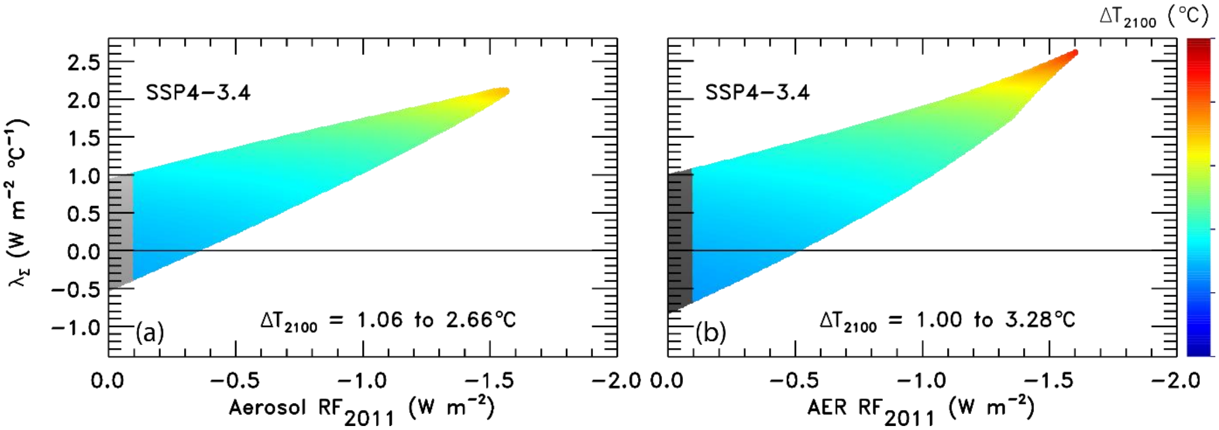

Figure S1. GMST anomaly in 2100 relative to pre-industrial (ΔT_{2100}) as a function of climate feedback parameter and AER RF_{2011} for two versions of the EM-GC. (a) The change in ΔT_{2100} for SSP4-3.4 using the original formulation of Eq. (2) where Q_{OCEAN} is subtracted outside of the feedback multiplicative term. (b) The change in ΔT_{2100} for SSP4-3.4 using the updated formulation of Eq. (2) where Q_{OCEAN} is subtracted within the feedback multiplicative term similar to Bony et al. (2006) and Schwartz (2012). The EM-GC is able to fit higher values of λ_{Σ} at strong aerosol cooling (around -1.5 W m^{-2}) for the new Eq. (2) compared to the original formulation in Canty et al. (2013) and Hope et al. (2017). The maximum value of future warming has increased due to the higher λ_{Σ} values.

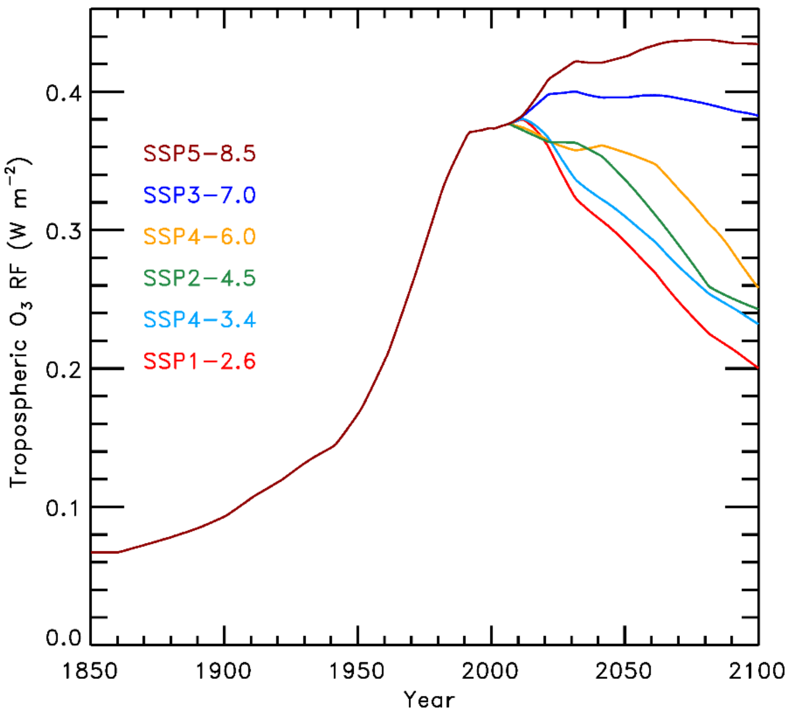

Figure S2. Radiative forcing of tropospheric ozone for the various SSPs analyzed in our study. The time series labeled SSP1-2.6, SSP2-4.5, SSP4-6.0, and SSP5-8.5 are from the corresponding RCP scenarios. We created the time series from SSP4-3.4 and SSP3-7.0 using linear combinations of the SSP1-2.6 and SSP5-8.5 time series.

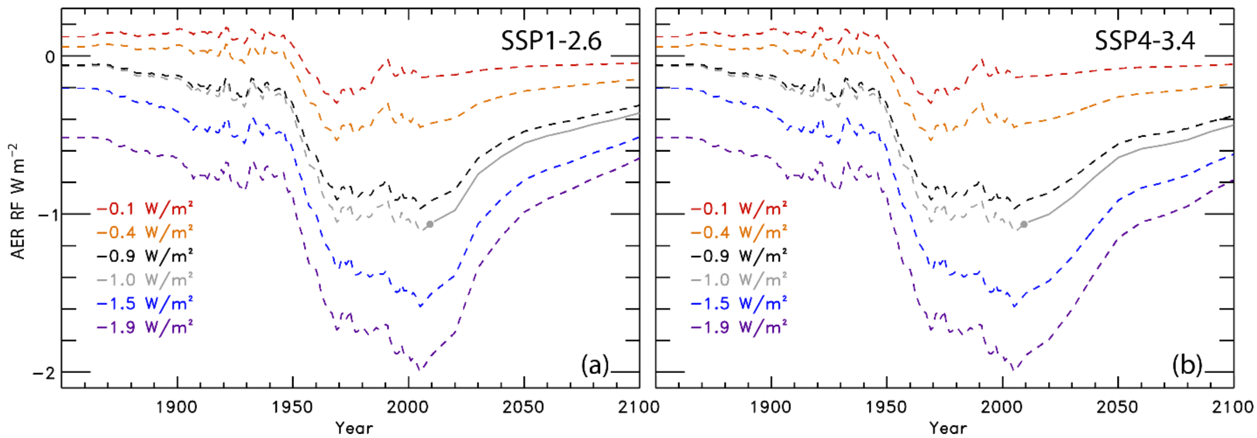

Figure S3. Radiative forcing time series due to tropospheric aerosols. (a) The RF time series due to tropospheric aerosols for SSP1-2.6. The solid grey circle denotes the value of AER RF_{2011} given by the SSP database. The solid grey lined labeled the −1.0 W m^{-2} time series is the AER RF time series given by the SSP database for SSP1-2.6. We appended a historical AER RF time series from the RCP scenarios and created five additional AER RF time series as described in Sect. 2.2.4. (b) Anthropogenic aerosol radiative forcing time series for SSP4-3.4.

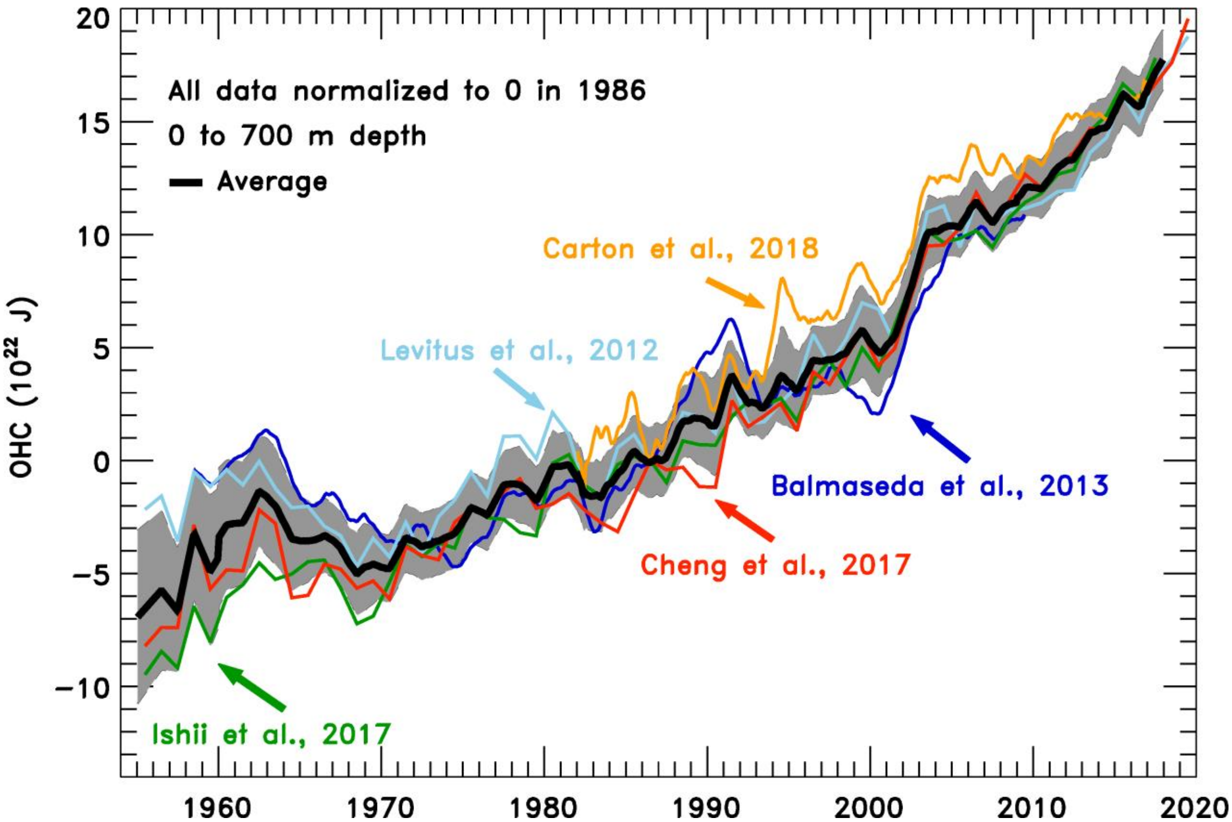

Figure S4. Ocean heat content time series. The five ocean heat content data records used in this analysis, normalized to the year 1986 because this year is in the middle of the average time series. The grey shaded region is the combined uncertainty estimate used in this analysis, centered around the average of the five data sets. The average of the ocean heat content records (1955 – 2017) is computed when there are three or more data sets available for a given year.

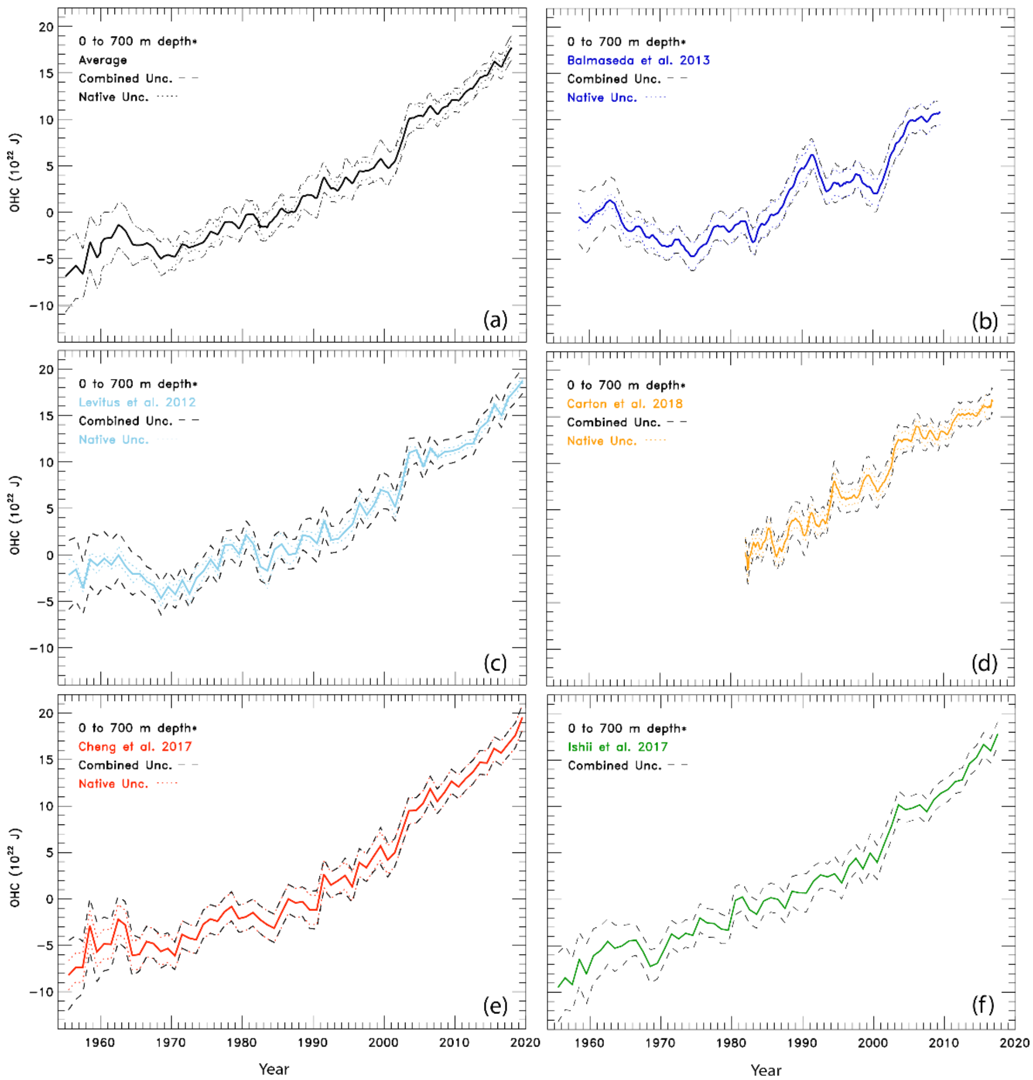

Figure S5. The ocean heat content records and uncertainty estimates analyzed in this study. (a) The average OHC record along with the standard deviation of the mean represented by the dotted black line, and the combined uncertainty of the standard deviation of the mean and the Cheng et al. (2017) estimates shown as the dashed black line. (b) Balmaseda OHC record with the standard deviation of the five ORSA ensemble members as the dotted line, and the combined uncertainty as the dashed line. (c) Levitus OHC record with the standard error as the native uncertainty, and the combined uncertainty. (d) Carton OHC record with the standard deviation of the mean of multiple ensemble members, and the combined uncertainty. (e) Cheng OHC record with the 1σ native uncertainty and the combined uncertainty. (f) Ishii OHC record with the combined uncertainty as the dashed line.

Table S1. Values of AAWR calculated using the EM-GC as a function of start and end year. The value of AAWR from 1975-2014 is shown in red. Each model run uses the best estimate of AER RF_{2011} (-0.9 W m^{-2}) and the average of five OHC records. The impact on varying the start and end year on AAWR is slight, except when a short record is used (i.e. 1984-2004, a 21 year span). A two-decade time span is not long enough to calculate an accurate estimate of AAWR. The value of AAWR is more sensitive to the choice of OHC or temperature record used.

		Start Year					
	AAWR (°C/decade)	**1970**	**1973**	**1975**	**1979**	**1982**	**1984**
End Year	**2004**	0.154 ± 0.006	0.153 ± 0.007	0.153 ± 0.008	0.145 ± 0.009	0.138 ± 0.010	0.130 ± 0.010
	2006	0.150 ± 0.006	0.149 ± 0.007	0.149 ± 0.008	0.141 ± 0.009	0.134 ± 0.009	0.126 ± 0.009
	2008	0.148 ± 0.006	0.146 ± 0.006	0.146 ± 0.007	0.138 ± 0.008	0.131 ± 0.008	0.124 ± 0.007
	2010	0.147 ± 0.005	0.145 ± 0.006	0.144 ± 0.007	0.137 ± 0.007	0.131 ± 0.007	0.125 ± 0.006
	2012	0.146 ± 0.005	0.144 ± 0.005	0.144 ± 0.006	0.137 ± 0.006	0.132 ± 0.006	0.128 ± 0.006
	2014	0.146 ± 0.004	0.145 ± 0.005	0.144 ± 0.005	0.139 ± 0.005	0.134 ± 0.006	0.130 ± 0.005
	2016	0.147 ± 0.004	0.145 ± 0.004	0.145 ± 0.005	0.140 ± 0.005	0.137 ± 0.005	0.134 ± 0.005
	2018	0.147 ± 0.003	0.146 ± 0.004	0.146 ± 0.004	0.142 ± 0.005	0.139 ± 0.005	0.137 ± 0.005

Table S2. Average values of AAWR calculated from the CMIP6 multi-model results using the regression method as a function of start and end year. The uncertainty corresponds to the 1σ standard deviation of AAWR found from the 50 GCMs. The value of AAWR from 1975-2014 is shown in red. The values of AAWR from the CMIP6 multi-model ensemble is more sensitive to the choice of start and end year than the EM-GC due to the small number of models. We use the same start and end year, 1975-2014, for the determination of AAWR for both the EM-GC and the CMIP6 multi-model ensemble for consistency.

		Start Year					
	AAWR (°C/decade)	**1970**	**1973**	**1975**	**1979**	**1982**	**1984**
End Year	**2004**	0.175	0.184	0.190	0.202	0.204	0.218
	2006	0.186	0.196	0.202	0.215	0.226	0.242
	2008	0.193	0.203	0.209	0.223	0.237	0.251
	2010	0.197	0.207	0.213	0.228	0.242	0.254
	2012	0.202	0.212	0.218	0.234	0.246	0.257
	2014	0.207	0.217	0.225	0.236	0.248	0.257

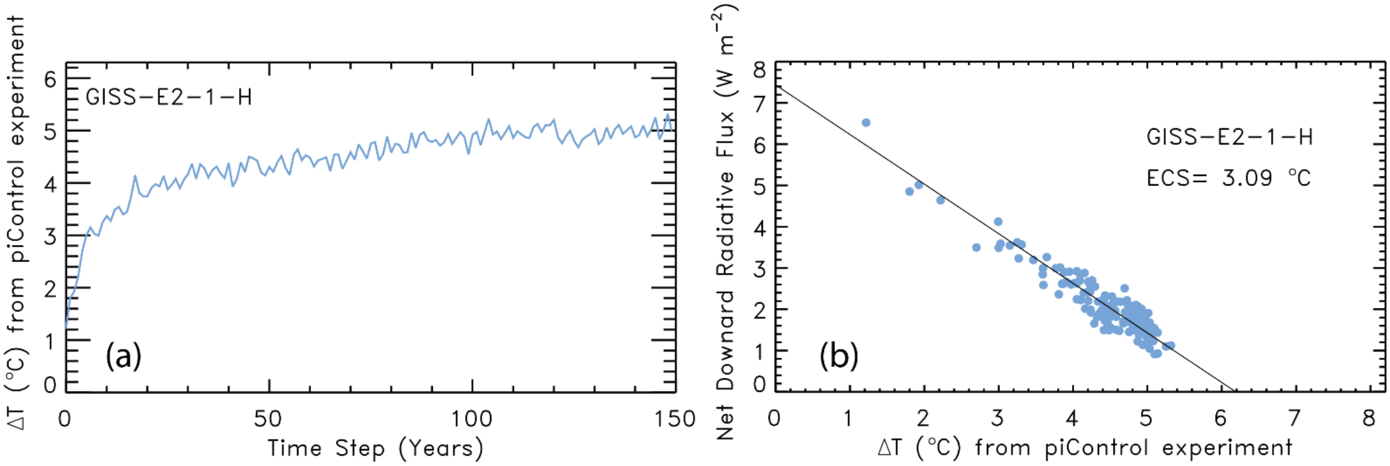

Figure S6. Steps for the Gregory et al. (2004) ECS calculation to compute ECS from the CMIP6 multi-model ensemble using GISS-E2-1-H (Kelley et al., 2020) as an example. (a) The change in Abrupt 4×CO_2 GMST (variable: tas) from the piControl experiment for 150 years. (b) Abrupt 4×CO_2 net downward radiative flux (variable: rtmt) versus the Abrupt 4×CO_2 GMST change from the piControl experiment for 150 years. The x-intercept of the orthogonal linear least squares fit of the GCM output divided by two yields the equilibrium climate sensitivity.

Table S3. Values of AAWR from 1975-2014 for the 50 CMIP6 multi-model Historical simulations available at time of the analysis (April 2020) for both the REG and LIN methods. The asterisk symbol (*) indicates there is only one run used to compute the value of AAWR for that GCM. No asterisk indicates the AAWR value shown in the table is the average of the values of AAWR for all runs of that model. The average ratio of LIN to REG for all 50 models is 1.04 ± 0.048, shown at the bottom of the table. The correlation coefficient (r^2) of 0.977 is also shown. We conclude our determination of AAWR from the CMIP6 multi-model ensemble is accurate to ±5%, which is much smaller than the difference between the CMIP6 multi-model ensemble values of AAWR and those found using the EM-GC framework.

Model	**AAWR, REG (°C/decade)**	**AAWR, LIN (°C/decade)**	**Model**	**AAWR, REG (°C/decade)**	**AAWR, LIN (°C/decade)**
ACCESS-CM2	0.212	0.216	GFDL-CM4*	0.238	0.250
ACCESS-ESM1-5	0.233	0.246	GFDL-ESM4	0.206	0.224
AWI-CM-1-1-MR	0.214	0.220	GISS-E2-1-G	0.192	0.198
BCC-CSM2-MR	0.214	0.228	GISS-E2-1-G-CC	0.200	0.213
BCC-ESM1	0.238	0.249	GISS-E2-1-H	0.234	0.244
CAMS-CSM1-0	0.130	0.138	HadGEM3-GC31-LL	0.277	0.292
CanESM5	0.349	0.361	HadGEM3-GC31-MM	0.225	0.234
CanESM5-CanOE	0.322	0.334	INM-CM4-8*	0.177	0.181
CAS-ESM2-0	0.191	0.204	INM-CM5-0	0.146	0.156
CESM2	0.234	0.243	IPSL-CM6A-LR	0.229	0.236
CESM2-FV2	0.213	0.158	KACE-1-0-G	0.250	0.260
CESM2-WACCM	0.266	0.291	MCM-UA-1-0	0.221	0.231
CESM2-WACCM-FV2	0.224	0.235	MIROC6	0.155	0.168
CIESM	0.244	0.251	MIROC-ES2L	0.161	0.167
CNRM-CM6-1	0.200	0.196	MPI-ESM1-2-HAM	0.173	0.186
CNRM-CM6-1-HR*	0.165	0.178	MPI-ESM1-2-HR	0.200	0.203
CNRM-ESM2-1	0.167	0.172	MPI-ESM1-2-LR	0.191	0.197
E3SM-1-0	0.263	0.278	MRI-ESM2-0	0.201	0.210
E3SM-1-1*	0.277	0.285	NESM3	0.242	0.253
E3SM-1-1-ECA*	0.272	0.274	NorCPM1	0.178	0.185
EC-Earth3*	0.291	0.310	NorESM2-LM	0.170	0.182
EC-Earth3-Veg*	0.216	0.223	NorESM2-MM*	0.150	0.154
FGOALS-f3-L	0.218	0.226	SAM0-UNICON*	0.241	0.250

FGOALS-g3	0.181	0.191	TaiESM1*	0.266	0.283
FIO-ESM-2-0	0.231	0.237	UKESM1-0-LL	0.294	0.312
Ratio = 1.04 ± 0.048			R^2 = 0.977		

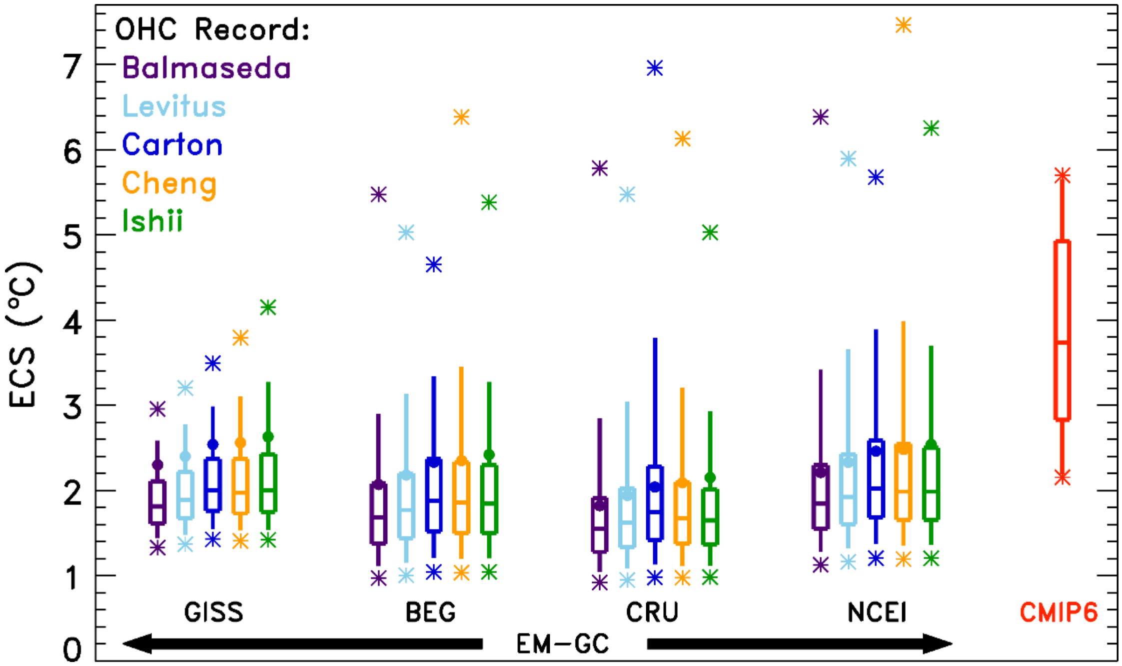

Figure S7. Values of ECS found using the EM-GC and the CMIP6 multi-model ensemble. Values of ECS utilizing the EM-GC are calculated using four temperature data sets and five ocean heat content records (as indicated). The box represents the 25th, 50th, and 75th percentiles of the values of ECS and the whiskers denote the 5th and 95th percentiles for the different OHC records and each temperature record without using the aerosol weighting method. The stars indicate the minimum and maximum values of ECS. The circles are the values of ECS associated with the best estimate of AER RF_{2011} of −0.9 W m^{-2}. The box labeled CMIP6 is the 25th, 50th, and 75th percentiles of the values of ECS from the CMIP6 multi-model ensemble, the whiskers indicate the 5th and 95th percentiles, and the stars represent the minimum and maximum values of ECS from the CMIP6 multi-model ensemble.

Table S4. Equilibrium climate sensitivity (ECS) from 28 CMIP6 GCMs. We can only calculate ECS for GCMs that provide Abrupt 4×CO_2 near surface air temperature (output variable: tas), net downward radiative flux (output variable: rtmt), and piControl near surface air temperature (output variable: tas) to the CMIP6 archive at time of the analysis (April 2020). All estimates are for one model run except for CanESM5, which is the average of two runs.

Model	ECS (K)
ACCESS-CM2	4.93
ACCESS-ESM1-5	3.63
BCC-CSM2-MR	3.16
BCC-ESM1	3.74
CanESM5	5.70
CESM2	5.32
CESM2-FV2	5.06
CESM2-WACCM	4.73
CESM2-WACCM-FV2	4.56
E3SM-1-0	5.28
EC-Earth3-Veg	4.34
GFDL-CM4	3.78
GFDL-ESM4	2.61
GISS-E2-1-G	2.71
GISS-E2-2-G	2.25
GISS-E2-1-H	3.09
HadGEM3-GC31-LL	5.65
INM-CM4-8	2.32
INM-CM5-0	2.39
IPSL-CM6A-LR	4.97
MCM-UA-1-0	3.68
MIROC6	2.84
MIROC-ES2L	2.83
NorESM2-LM	2.19
NorESM2-MM	2.15
SAM0-UNICON	3.53
TaiESM1	4.33
UKESM1-0-LL	5.40

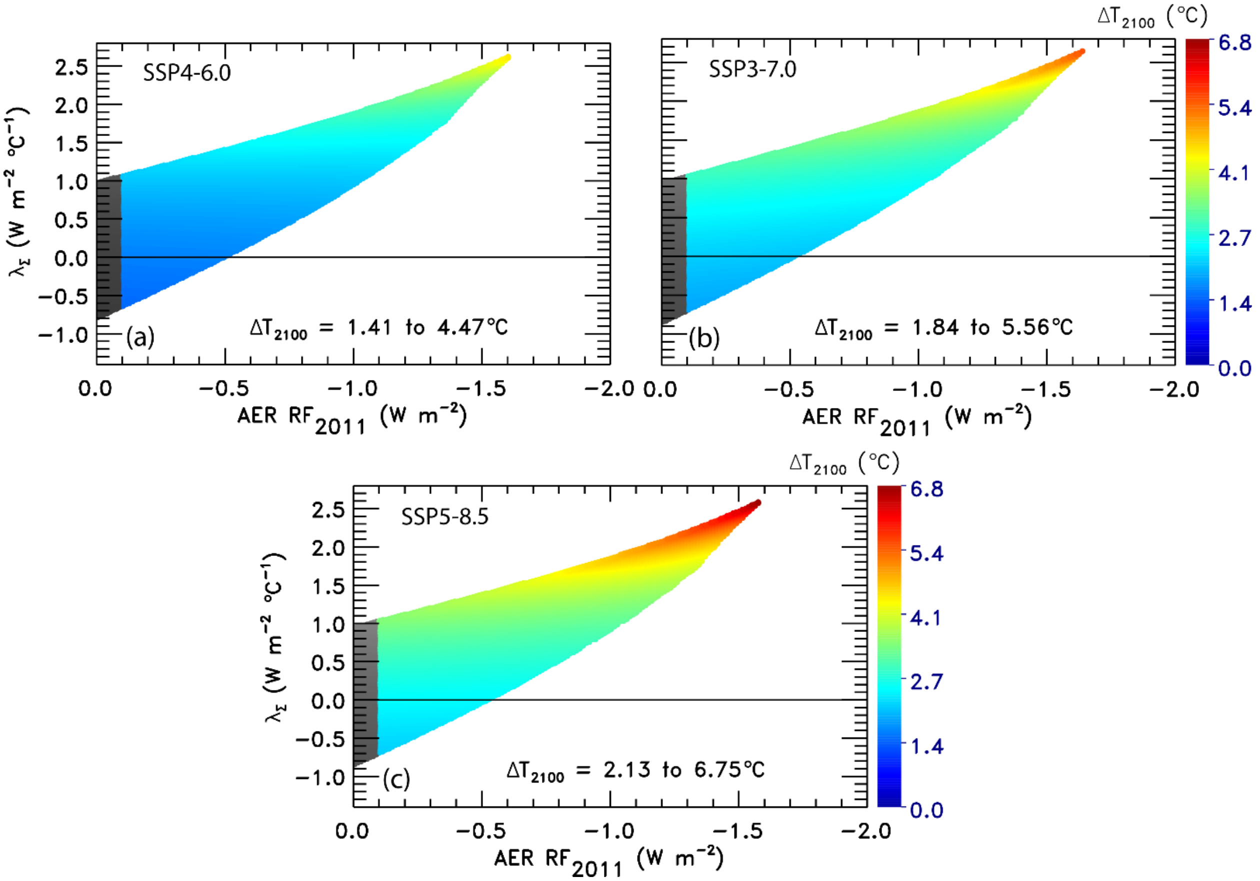

Figure S8. GMST anomaly in 2100 from pre-industrial (ΔT_{2100}) as a function of climate feedback parameter and AER RF_{2011}. (a) ΔT for SSP4-6.0. The region outside of the tropospheric aerosol radiative forcing rage provided by IPCC 2013 (Myhre et al., 2013) is shaded grey. Colors denote the change in ΔT_{2100}. (b) ΔT_{2100} for SSP3-7.0. (c) ΔT_{2100} for SSP5-8.5.

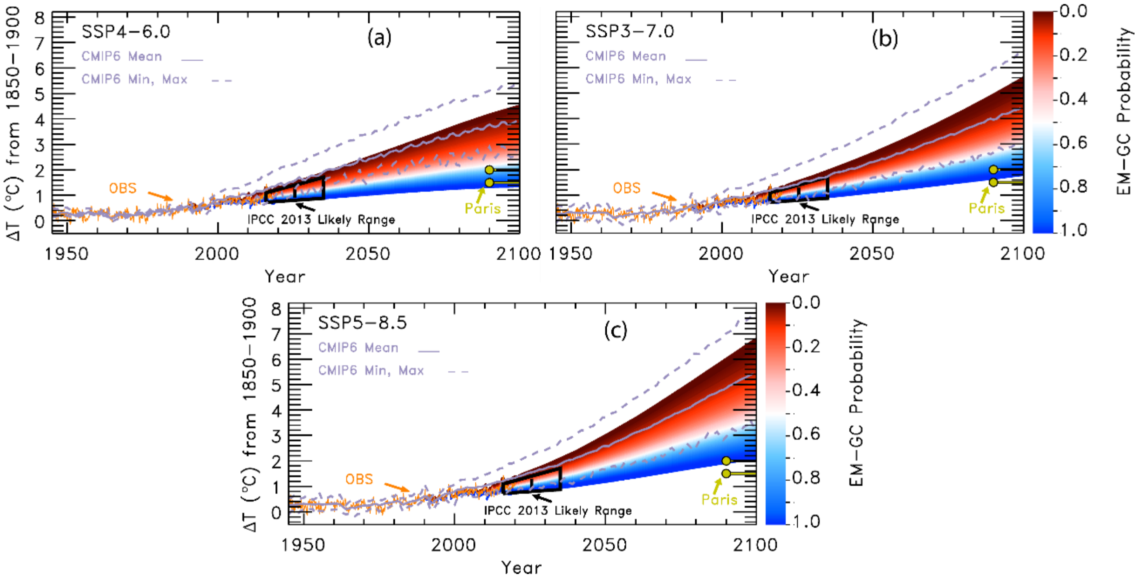

Figure S9. Probabilistic forecasts of future projections of ΔT using the EM-GC for the SSP4-6.0, SSP3-7.0, and SSP5-8.5 scenarios. (a) Future projections of ΔT for SSP4-6.0. Observations (orange) are from CRU. The IPCC 2013 likely range of warming (black) is from Figure 11.25b of chapter 11 of the IPCC 2013 report. The Paris Agreement target and upper limit (yellow) are shown for comparison to projections of ΔT using the EM-GC. The CMIP6 minimum, multi-model mean, and maximum values of the rise in ΔT are shown to compare to projections from the EM-GC. Colors denote the probability of reaching at least that temperature by the end of the century and are computed using the aerosol weighting method (see Sect. 2.5). (b) Future projections of ΔT for SSP3-7.0. (c) Future projections of ΔT for SSP5-8.5.

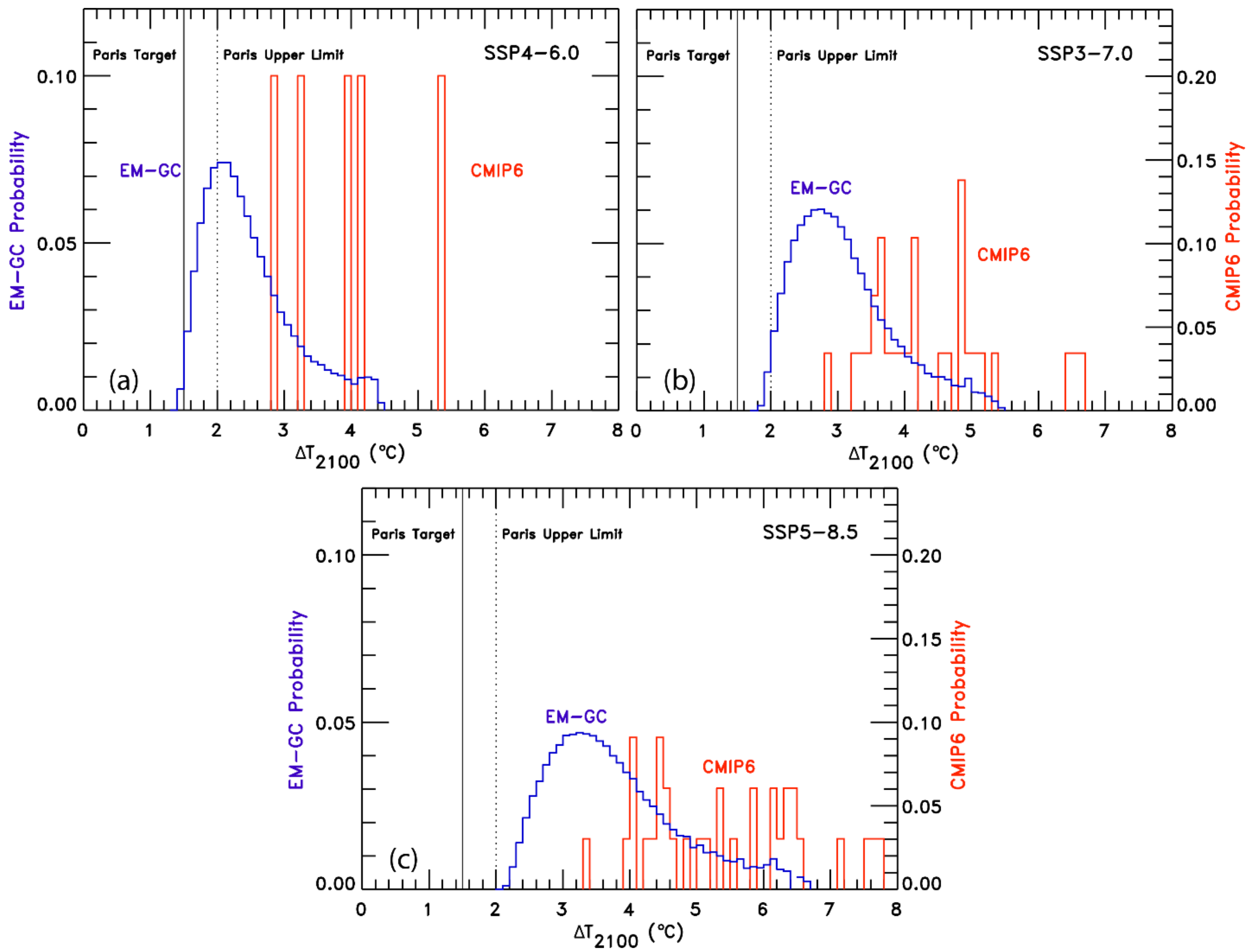

Figure S10. Probability density functions (PDF) for the increase in ΔT_{2100} using the EM-GC and the CMIP6 multi-model ensemble. (a) PDF for EM-GC (blue) results and CMIP6 multi-model results (red) for SSP4-6.0. The left-hand y-axis is for EM-GC probabilities and the righthand y-axis is for GCM probabilities. (b) PDF for SSP3-7.0. (c) PDF for SSP5-8.5.

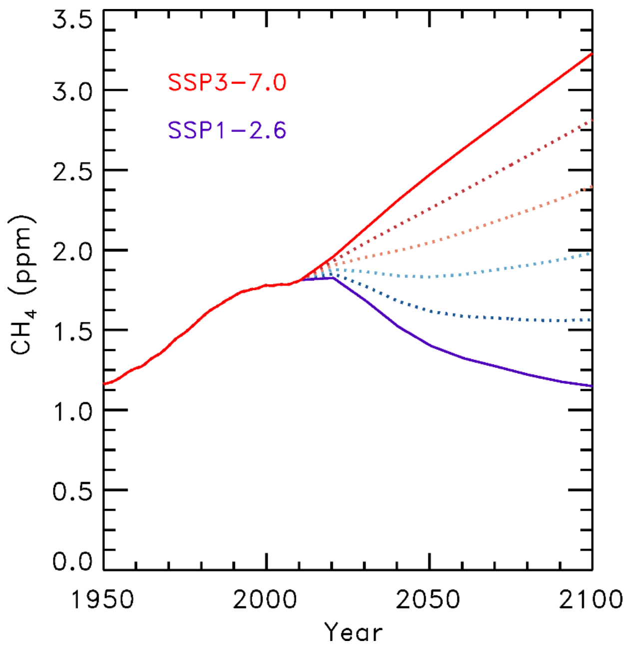

Figure S11. Blended methane mixing ratios. The dotted lines are linear combinations of the time series of methane abundances using SSP1-2.6 and SSP3-7.0 to span the range of values of future methane. The solid lines are the SSP1-2.6 and SSP3-7.0 methane mixing ratio time series.

Table S5. Details of the CMIP6 GCMs used in this study.

Institution	Model	Model Output
AS-RCEC	TaiESM1	No reference provided
AWI	AWI-CM-1-1-MR	(Semmler et al., 2018a, 2018b, 2018c, 2019a, 2019b)
BCC	BCC-CSM2-MR	(Wu et al., 2018a, 2018b, 2018c; Xin et al., 2019a, 2019b, 2019c, 2019d)
	BCC-ESM1	(Zhang et al., 2018a, 2018b, 2019)
CAMS	CAMS-CSM1-0	(Rong, 2019a, 2019b, 2019c, 2019d, 2019e, 2019f)
CAS	CAS-ESM2-0	(Chai, 2019)
	FGOALS-f3-L	(YU, 2019a, 2019b, 2019c, 2019d, 2019e)
	FGOALS-g3	(Li, 2019a, 2019b, 2019c, 2019d, 2019e)
CCCma	CanESM5	(Swart et al., 2019f, 2019g, 2019h, 2019i, 2019j, 2019k, 2019l, 2019m, 2019n, 2019o)
	CanESM5-CanOE	(Swart et al., 2019a, 2019b, 2019c, 2019d, 2019e)
CNRM-CERFACS	CNRM-CM6-1	(Voldoire, 2018, 2019c, 2019d, 2019e, 2019f)
	CNRM-CM6-1-HR	(Voldoire, 2019a, 2019b, 2020a, 2020b)
	CNRM-ESM2-1	(Seferian, 2018; Voldoire, 2019g, 2019h, 2019i, 2019j, 2019k, 2019l)
CSIRO	ACCESS-ESM1-5	(Ziehn et al., 2019a, 2019b, 2019c, 2019d, 2019e, 2019f, 2019g)
CSIRO-ARCCSS	ACCESS-CM2	(Dix et al., 2019a, 2019b, 2019c, 2019d, 2019e, 2019f, 2019g)
E3SM-Project	E3SM-1-0	(Bader et al., 2018, 2019a, 2019b)
	E3SM-1-1-ECA	(Bader et al., 2020)
E3SM-Project RUBISCO	E3SM-1-1	(Bader et al., 2019c)
EC-Earth-Consortium	EC-Earth3	(EC-Earth Consortium (EC-Earth), 2019i, 2019j, 2019k, 2019l, 2019m)
	EC-Earth3-Veg	(EC-Earth Consortium (EC-Earth), 2019a, 2019b, 2019c, 2019d, 2019e, 2019f, 2019g, 2019h)

FIO-QLNM	FIO-ESM-2-0	(Song et al., 2019a, 2019b, 2019c, 2019d)
HAMMOZ-Consortium	MPI-ESM1-2-HAM	(Neubauer et al., 2019)
INM	INM-CM4-8	(Volodin et al., 2019a, 2019b, 2019c, 2019d, 2019e, 2019f, 2019g)
	INM-CM5-0	(Volodin et al., 2019m, 2019h, 2019n, 2019i, 2019j, 2019k, 2019l)
IPSL	IPSL-CM6A-LR	(Boucher et al., 2018a, 2018b, 2018c, 2019a, 2019b, 2019c, 2019d, 2019e, 2019f, 2019g)
MIROC	MIROC6	(Shiogama et al., 2019a, 2019b, 2019c, 2019d, 2019e, 2019f, 2019g; Tatebe and Watanabe, 2018a, 2018b, 2018c)
	MIROC-ES2L	(Hajima et al., 2019; Tachiiri et al., 2019a, 2019b, 2019c, 2019d, 2019e)
MOHC	HadGEM3-GC31-MM	(Ridley et al., 2019c)
MOHC NERC	HadGEM3-GC31-LL	(Good, 2019, 2020a, 2020b; Ridley et al., 2018, 2019a, 2019b)
MOHC, NERC, NIMS-KMA, NIWA	UKESM1-0-LL	(Byun, 2020; Good et al., 2019a, 2019b, 2019c, 2019d, 2019e, 2019f; Tang et al., 2019a, 2019b, 2019c)
MPI-M AWI	MPI-ESM1-2-LR	(Wieners et al., 2019a, 2019b, 2019c, 2019d, 2019e)
MPI-M DWD DKRZ	MPI-ESM1-2-HR	(Jungclaus et al., 2019; Schupfner et al., 2019a, 2019b, 2019c, 2019d; Steger et al., 2019)
MRI	MRI-ESM2-0	(Yukimoto et al., 2019a, 2019b, 2019c, 2019d, 2019e, 2019f, 2019g, 2019h)
NASA-GISS	GISS-E2-1-G	(NASA Goddard Institute for Space Studies (NASA/GISS), 2018a, 2018b, 2018c, 2020a, 2020b, 2020c, 2020d)
	GISS-E2-1-G-CC	No reference provided
	GISS-E2-2-G	(NASA Goddard Institute for Space Studies (NASA/GISS), 2019a)
	GISS-E2-1-H	(NASA Goddard Institute for Space Studies (NASA/GISS), 2018d, 2019b, 2019c)
NCAR	CESM2-WACCM-FV2	(Danabasoglu, 2019d, 2019e, 2020a)

	CESM2	(Danabasoglu, 2019c, 2019d, 2019e, 2019f, 2019g, 2019h; Danabasoglu et al., 2019)
	CESM2-FV2	(Danabasoglu, 2019b, 2019c, 2020b)
	CESM2-WACCM	(Danabasoglu, 2019f, 2019g, 2019h, 2019a, 2019i, 2019j, 2019k)
	NorCPM1	(Bethke et al., 2019a, 2019b, 2019c)
NCC	NorESM2-LM	(Seland et al., 2019a, 2019b, 2019c, 2019d, 2019e, 2019f, 2019g)
	NorESM2-MM	(Bentsen et al., 2019a, 2019b, 2019c, 2019d, 2019e, 2019f, 2019g)
NIMS-KMA	KACE-1-0-G	(Byun et al., 2019a, 2019b, 2019c, 2019d, 2019e)
NOAA-GFDL	GFDL-CM4	(Guo et al., 2018a, 2018b, 2018c, 2018d, 2018e)
	GFDL-ESM4	(John et al., 2018a, 2018b, 2018c, 2018d, 2018e; Krasting et al., 2018a, 2018b, 2018c)
NUIST	NESM3	(Cao, 2019a, 2019b, 2019c; Cao and Wang, 2019)
SNU	SAM0-UNICON	(Park and Shin, 2019a, 2019b, 2019c)
THU	CIESM	(Huang, 2019a, 2019b, 2020a, 2020b)
UA	MCM-UA-1-0	(Stouffer, 2019a, 2019b, 2019c, 2019d, 2019e, 2019f, 2019g)

References

Bader, D. C., Leung, R., Taylor, M. and McCoy, R. B.: E3SM-Project E3SM1.0 model output prepared for CMIP6 CMIP piControl, Earth System Grid Federation, , doi:https://doi.org/10.22033/ESGF/CMIP6.4499, 2018.

Bader, D. C., Leung, R., Taylor, M. and McCoy, R. B.: E3SM-Project E3SM1.0 model output prepared for CMIP6 CMIP abrupt-4xCO2, Earth System Grid Federation, , doi:https://doi.org/10.22033/ESGF/CMIP6.4491, 2019a.

Bader, D. C., Leung, R., Taylor, M. and McCoy, R. B.: E3SM-Project E3SM1.0 model output prepared for CMIP6 CMIP historical, Earth System Grid Federation, , doi:https://doi.org/10.22033/ESGF/CMIP6.4497, 2019b.

Bader, D. C., Leung, R., Taylor, M. and McCoy, R. B.: E3SM-Project E3SM1.1 model output prepared for CMIP6 CMIP historical, Earth System Grid Federation, , doi:https://doi.org/10.22033/ESGF/CMIP6.11485, 2019c.

Bader, D. C., Leung, R., Taylor, M. and McCoy, R. B.: E3SM-Project E3SM1.1ECA model output prepared for CMIP6 CMIP historical, Earth System Grid Federation, , doi:https://doi.org/10.22033/ESGF/CMIP6.11486, 2020.

Balmaseda, M. A., Trenberth, K. E. and Källén, E.: Distinctive climate signals in reanalysis of global ocean heat content, Geophys. Res. Lett., 40(9), 1754–1759, doi:10.1002/grl.50382, 2013a.

Balmaseda, M. A., Mogensen, K. and Weaver, A. T.: Evaluation of the ECMWF ocean reanalysis system ORAS4, Q. J. R. Meteorol. Soc., 139(674), 1132–1161, doi:10.1002/qj.2063, 2013b.

Bentsen, M., Oliviè, D. J. L., Seland, Ø., Toniazzo, T., Gjermundsen, A., Graff, L. S., Debernard, J. B., Gupta, A. K., He, Y., Kirkevåg, A., Schwinger, J., Tjiputra, J., Aas, K. S., Bethke, I., Fan, Y., Griesfeller, J., Grini, A., Guo, C., Ilicak, M., Karset, I. H. H., Landgren, O. A., Liakka, J., Moseid, K. O., Nummelin, A., Spensberger, C., Tang, H., Zhang, Z., Heinze, C., Iversen, T. and Schulz, M.: NCC NorESM2-MM model output prepared for CMIP6 CMIP abrupt-4xCO2, Earth System Grid Federation, , doi:https://doi.org/10.22033/ESGF/CMIP6.7840, 2019a.

Bentsen, M., Oliviè, D. J. L., Seland, Ø., Toniazzo, T., Gjermundsen, A., Graff, L. S., Debernard, J. B., Gupta, A. K., He, Y., Kirkevåg, A., Schwinger, J., Tjiputra, J., Aas, K. S., Bethke, I., Fan, Y., Griesfeller, J., Grini, A., Guo, C., Ilicak, M., Karset, I. H. H., Landgren, O. A., Liakka, J., Moseid, K. O., Nummelin, A., Spensberger, C., Tang, H., Zhang, Z., Heinze, C., Iversen, T. and Schulz, M.: NCC NorESM2-MM model output prepared for CMIP6 CMIP historical, Earth System Grid Federation, , doi:https://doi.org/10.22033/ESGF/CMIP6.8040, 2019b.

Bentsen, M., Oliviè, D. J. L., Seland, Ø., Toniazzo, T., Gjermundsen, A., Graff, L. S., Debernard, J. B., Gupta, A. K., He, Y., Kirkevåg, A., Schwinger, J., Tjiputra, J., Aas, K. S., Bethke, I., Fan, Y., Griesfeller, J., Grini, A., Guo, C., Ilicak, M., Karset, I. H. H., Landgren, O. A., Liakka, J., Moseid, K. O., Nummelin, A., Spensberger, C., Tang, H., Zhang, Z., Heinze, C., Iversen, T. and Schulz, M.: NCC NorESM2-MM model output prepared for CMIP6 CMIP piControl, Earth System Grid Federation, , doi:https://doi.org/10.22033/ESGF/CMIP6.8221, 2019c.

Bentsen, M., Oliviè, D. J. L., Seland, Ø., Toniazzo, T., Gjermundsen, A., Graff, L. S., Debernard, J. B., Gupta, A. K., He, Y., Kirkevåg, A., Schwinger, J., Tjiputra, J., Aas, K. S., Bethke, I., Fan, Y., Griesfeller, J., Grini, A., Guo, C., Ilicak, M., Karset, I. H. H., Landgren, O. A., Liakka, J., Moseid, K. O., Nummelin, A., Spensberger, C., Tang, H., Zhang, Z., Heinze, C., Iversen, T. and Schulz, M.: NCC NorESM2-MM model output prepared for CMIP6 ScenarioMIP ssp126, Earth System Grid Federation, , doi:https://doi.org/10.22033/ESGF/CMIP6.8250, 2019d.

Bentsen, M., Oliviè, D. J. L., Seland, Ø., Toniazzo, T., Gjermundsen, A., Graff, L. S., Debernard, J. B., Gupta, A. K., He, Y., Kirkevåg, A., Schwinger, J., Tjiputra, J., Aas, K. S., Bethke, I., Fan, Y., Griesfeller, J., Grini, A., Guo, C., Ilicak, M., Karset, I. H. H., Landgren, O. A., Liakka, J., Moseid, K. O., Nummelin, A., Spensberger, C., Tang, H., Zhang, Z., Heinze, C., Iversen, T. and Schulz, M.: NCC NorESM2-MM model output prepared for CMIP6 ScenarioMIP ssp245, Earth System Grid Federation, , doi:https://doi.org/10.22033/ESGF/CMIP6.8255, 2019e.

Bentsen, M., Oliviè, D. J. L., Seland, Ø., Toniazzo, T., Gjermundsen, A., Graff, L. S., Debernard, J. B., Gupta, A. K., He, Y., Kirkevåg, A., Schwinger, J., Tjiputra, J., Aas, K. S., Bethke, I., Fan, Y., Griesfeller, J., Grini, A., Guo, C., Ilicak, M., Karset, I. H. H., Landgren, O. A., Liakka, J., Moseid, K. O., Nummelin, A., Spensberger, C., Tang, H., Zhang, Z., Heinze, C., Iversen, T. and Schulz, M.: NCC NorESM2-MM model output prepared for CMIP6 ScenarioMIP ssp370, Earth System Grid Federation, , doi:https://doi.org/10.22033/ESGF/CMIP6.8270, 2019f.

Bentsen, M., Oliviè, D. J. L., Seland, Ø., Toniazzo, T., Gjermundsen, A., Graff, L. S., Debernard, J. B., Gupta, A. K., He, Y., Kirkevåg, A., Schwinger, J., Tjiputra, J., Aas, K. S., Bethke, I., Fan, Y., Griesfeller, J., Grini, A., Guo, C., Ilicak, M., Karset, I. H. H., Landgren, O. A., Liakka, J., Moseid, K. O., Nummelin, A., Spensberger, C., Tang, H., Zhang, Z., Heinze, C., Iversen, T. and Schulz, M.: NCC NorESM2-MM model output prepared for CMIP6 ScenarioMIP ssp585, Earth System Grid Federation, , doi:https://doi.org/10.22033/ESGF/CMIP6.8321, 2019g.

Bethke, I., Wang, Y., Counillon, F., Kimmritz, M., Fransner, F., Samuelsen, A., Langehaug, H. R., Chiu, P.-G., Bentsen, M., Guo, C., Tjiputra, J., Kirkevåg, A., Oliviè, D. J. L., Seland, Ø., Fan, Y., Lawrence, P., Eldevik, T. and Keenlyside, N.: NCC NorCPM1 model output prepared for CMIP6 CMIP abrupt-4xCO2, Earth System Grid Federation, , doi:https://doi.org/10.22033/ESGF/CMIP6.10862, 2019a.

Bethke, I., Wang, Y., Counillon, F., Kimmritz, M., Fransner, F., Samuelsen, A., Langehaug, H. R., Chiu, P., Bentsen, M., Guo, C., Tjiputra, J., Kirkevåg, A., Oliviè, D. J. L., Seland, Ø., Fan, Y., Lawrence, P., Eldevik, T. and Keenlyside, N.: NCC NorCPM1 model output prepared for CMIP6 CMIP historical, Earth System Grid Federation, , doi:https://doi.org/10.22033/ESGF/CMIP6.10894, 2019b.

Bethke, I., Wang, Y., Counillon, F., Kimmritz, M., Fransner, F., Samuelsen, A., Langehaug, H. R., Chiu, P.-G., Bentsen, M., Guo, C., Tjiputra, J., Kirkevåg, A., Oliviè, D. J. L., Seland, Ø., Fan, Y., Lawrence, P., Eldevik, T. and Keenlyside, N.: NCC NorCPM1 model output prepared for CMIP6 CMIP piControl, Earth System Grid Federation, , doi:https://doi.org/10.22033/ESGF/CMIP6.10896, 2019c.

Bony, S., Colman, R., Kattsov, V. M., Allan, R. P., Bretherton, C. S., Dufresne, J. L., Hall, A., Hallegatte, S., Holland, M. M., Ingram, W., Randall, D. A., Soden, B. J., Tselioudis, G. and Webb, M. J.: How well do we understand and evaluate climate change feedback processes?, J. Clim., 19(15), 3445–3482, doi:10.1175/JCLI3819.1, 2006.

Boucher, O., Denvil, S., Caubel, A. and Foujols, M. A.: IPSL IPSL-CM6A-LR model output prepared for CMIP6 CMIP abrupt-4xCO2, Earth System Grid Federation, , doi:https://doi.org/10.22033/ESGF/CMIP6.5109, 2018a.

Boucher, O., Denvil, S., Caubel, A. and Foujols, M. A.: IPSL IPSL-CM6A-LR model output prepared for CMIP6 CMIP historical, Earth System Grid Federation, , doi:https://doi.org/10.22033/ESGF/CMIP6.5195, 2018b.

Boucher, O., Denvil, S., Caubel, A. and Foujols, M. A.: IPSL IPSL-CM6A-LR model output prepared for CMIP6 CMIP piControl, Earth System Grid Federation, , doi:https://doi.org/10.22033/ESGF/CMIP6.5251, 2018c.

Boucher, O., Denvil, S., Caubel, A. and Foujols, M. A.: IPSL IPSL-CM6a-LR model output prepared for CMIP6 ScenarioMIP ssp119, Earth System Grid Federation, , doi:https://doi.org/10.22033/ESGF/CMIP6.5261, 2019a.

Boucher, O., Denvil, S., Caubel, A. and Foujols, M. A.: IPSL IPSL-CM6A-LR model output prepared for CMIP6 ScenarioMIP ssp126, Earth System Grid Federation, , doi:https://doi.org/10.22033/ESGF/CMIP6.5262, 2019b.

Boucher, O., Denvil, S., Caubel, A. and Foujols, M. A.: IPSL IPSL-CM6A-LR model output prepared for CMIP6 ScenarioMIP ssp370, Earth System Grid Federation, , doi:https://doi.org/10.22033/ESGF/CMIP6.5265, 2019c.

Boucher, O., Denvil, S., Caubel, A. and Foujols, M. A.: IPSL IPSL-CM6A-LR model output prepared for CMIP6 ScenarioMIP ssp434, Earth System Grid Federation, , doi:https://doi.org/10.22033/ESGF/CMIP6.5267, 2019d.

Boucher, O., Denvil, S., Caubel, A. and Foujols, M. A.: IPSL IPSL-CM6A-LR model output prepared for CMIP6 ScenarioMIP ssp460, Earth System Grid Federation, , doi:https://doi.org/10.22033/ESGF/CMIP6.5268, 2019e.

Boucher, O., Denvil, S., Caubel, A. and Foujols, M. A.: IPSL IPSL-CM6A-LR model output prepared for CMIP6 ScenarioMIP ssp585, Earth System Grid Federation, , doi:https://doi.org/10.22033/ESGF/CMIP6.5271, 2019f.

Boucher, O., Denvil, S., Caubel, A. and Foujols, M. A.: PSL IPSL-CM6A-LR model output prepared for CMIP6 ScenarioMIP ssp245, Earth System Grid Federation, , doi:https://doi.org/10.22033/ESGF/CMIP6.5264, 2019g.

Byun, Y.-H.: NIMS-KMA UKESM1.0-LL model output prepared for CMIP6 CMIP historical, Earth System Grid Federation, , doi:https://doi.org/10.22033/ESGF/CMIP6.8379, 2020.

Byun, Y.-H., Lim, Y.-J., Sung, H. M., Kim, J., Sun, M. and Kim, B.-H.: NIMS-KMA KACE1.0-G model output prepared for CMIP6 CMIP historical, Earth System Grid Federation, , doi:https://doi.org/10.22033/ESGF/CMIP6.8378, 2019a.

Byun, Y.-H., Lim, Y.-J., Shim, S., Sung, H. M., Sun, M., Kim, J., Kim, B.-H., Lee, J.-H. and Moon, H.: NIMS-KMA KACE1.0-G model output prepared for CMIP6 ScenarioMIP ssp126, Earth System Grid Federation, , doi:https://doi.org/10.22033/ESGF/CMIP6.8432, 2019b.

Byun, Y.-H., Lim, Y.-J., Shim, S., Sung, H. M., Sun, M., Kim, J., Kim, B.-H., Lee, J.-H. and Moon, H.: NIMS-KMA KACE1.0-G model output prepared for CMIP6 ScenarioMIP ssp245, Earth System Grid Federation, , doi:https://doi.org/10.22033/ESGF/CMIP6.8435, 2019c.

Byun, Y.-H., Lim, Y.-J., Shim, S., Sung, H. M., Sun, M., Kim, J., Kim, B.-H., Lee, J.-H. and Moon, H.: NIMS-KMA KACE1.0-G model output prepared for CMIP6 ScenarioMIP ssp370, Earth System Grid Federation, , doi:https://doi.org/10.22033/ESGF/CMIP6.8437, 2019d.

Byun, Y.-H., Lim, Y.-J., Shim, S., Sung, H. M., Sun, M., Kim, J., Kim, B.-H., Lee, J.-H. and Moon, H.: NIMS-KMA KACE1.0-G model output prepared for CMIP6 ScenarioMIP ssp585, Earth System Grid Federation, , doi:https://doi.org/10.22033/ESGF/CMIP6.8456, 2019e.

Canty, T., Mascioli, N. R., Smarte, M. D. and Salawitch, R. J.: An empirical model of global climate – Part 1: A critical evaluation of volcanic cooling, Atmos. Chem. Phys., 13(8), 3997–4031, doi:10.5194/acp-13-3997-2013, 2013.

Cao, J.: NUIST NESMv3 model output prepared for CMIP6 ScenarioMIP ssp126, Earth System Grid Federation, , doi:https://doi.org/10.22033/ESGF/CMIP6.8780, 2019a.

Cao, J.: NUIST NESMv3 model output prepared for CMIP6 ScenarioMIP ssp245, Earth System Grid Federation, , doi:https://doi.org/10.22033/ESGF/CMIP6.8781, 2019b.

Cao, J.: NUIST NESMv3 model output prepared for CMIP6 ScenarioMIP ssp585, Earth System Grid Federation, , doi:https://doi.org/10.22033/ESGF/CMIP6.8790, 2019c.

Cao, J. and Wang, B.: NUIST NESMv3 model output prepared for CMIP6 CMIP historical, , doi:https://doi.org/10.22033/ESGF/CMIP6.8769, 2019.

Carton, J. A., Chepurin, G. A. and Chen, L.: SODA3: A New Ocean Climate Reanalysis, J. Clim., 31(17), 6967–6983, doi:10.1175/jcli-d-18-0149.1, 2018.

Chai, Z.: CAS CAS-ESM1.0 model output prepared for CMIP6 CMIP historical, Earth System Grid Federation, , doi:https://doi.org/10.22033/ESGF/CMIP6.3353, 2019.

Cheng, L., Trenberth, K. E., Fasullo, J., Boyer, T., Abraham, J. and Zhu, J.: Improved estimates of ocean heat content from 1960 to 2015, Sci. Adv., 3(3), 1–11, doi:10.1126/sciadv.1601545, 2017.

Danabasoglu, G.: NCAR CESM-WACCM model output prepared for CMIP6 ScenarioMIP ssp126, Earth System Grid Federation, , doi:https://doi.org/10.22033/ESGF/CMIP6.10100, 2019a.

Danabasoglu, G.: NCAR CESM2-FV2 model output prepared for CMIP6 CMIP historical, Earth System Grid Federation, , doi:https://doi.org/10.22033/ESGF/CMIP6.11297, 2019b.

Danabasoglu, G.: NCAR CESM2-FV2 model output prepared for CMIP6 CMIP piControl, Earth System Grid Federation, , doi:https://doi.org/10.22033/ESGF/CMIP6.11301, 2019c.

Danabasoglu, G.: NCAR CESM2-WACCM-FV2 model output prepared for CMIP6 CMIP historical, Earth System Grid Federation, , doi:https://doi.org/10.22033/ESGF/CMIP6.11298, 2019d.

Danabasoglu, G.: NCAR CESM2-WACCM-FV2 model output prepared for CMIP6 CMIP piControl, Earth System Grid Federation, , doi:https://doi.org/10.22033/ESGF/CMIP6.11302, 2019e.

Danabasoglu, G.: NCAR CESM2-WACCM model output prepared for CMIP6 CMIP abrupt-4xCO2, Earth System Grid Federation, , doi:https://doi.org/10.22033/ESGF/CMIP6.10039, 2019f.

Danabasoglu, G.: NCAR CESM2-WACCM model output prepared for CMIP6 CMIP historical, Earth System Grid Federation, , doi:https://doi.org/10.22033/ESGF/CMIP6.10071, 2019g.

Danabasoglu, G.: NCAR CESM2-WACCM model output prepared for CMIP6 CMIP piControl, Earth System Grid Federation, , doi:https://doi.org/10.22033/ESGF/CMIP6.10094, 2019h.

Danabasoglu, G.: NCAR CESM2-WACCM model output prepared for CMIP6 ScenarioMIP ssp245, Earth System Grid Federation, , doi:https://doi.org/10.22033/ESGF/CMIP6.10101, 2019i.

Danabasoglu, G.: NCAR CESM2-WACCM model output prepared for CMIP6 ScenarioMIP ssp370, Earth System Grid Federation, , doi:https://doi.org/10.22033/ESGF/CMIP6.10102, 2019j.

Danabasoglu, G.: NCAR CESM2-WACCM model output prepared for CMIP6 ScenarioMIP ssp585, Earth System Grid Federation, , doi:https://doi.org/10.22033/ESGF/CMIP6.10115, 2019k.

Danabasoglu, G.: NCAR CESM2 model output prepared for CMIP6 CMIP abrupt-4xCO2, Earth System Grid Federation, , doi:https://doi.org/10.22033/ESGF/CMIP6.7519, 2019l.

Danabasoglu, G.: NCAR CESM2 model output prepared for CMIP6 CMIP historical, Earth System Grid Federation, , doi:https://doi.org/10.22033/ESGF/CMIP6.7627, 2019m.

Danabasoglu, G.: NCAR CESM2 model output prepared for CMIP6 ScenarioMIP ssp126, Earth System Grid Federation, , doi:https://doi.org/10.22033/ESGF/CMIP6.7746, 2019n.

Danabasoglu, G.: NCAR CESM2 model output prepared for CMIP6 ScenarioMIP ssp245, Earth System Grid Federation, , doi:https://doi.org/10.22033/ESGF/CMIP6.7748, 2019o.

Danabasoglu, G.: NCAR CESM2 model output prepared for CMIP6 ScenarioMIP ssp370, Earth System Grid Federation, , doi:https://doi.org/10.22033/ESGF/CMIP6.7753, 2019p.

Danabasoglu, G.: NCAR CESM2 model output prepared for CMIP6 ScenarioMIP ssp585, Earth System Grid Federation, , doi:https://doi.org/10.22033/ESGF/CMIP6.7768, 2019q.

Danabasoglu, G.: CAR CESM2-WACCM-FV2 model output prepared for CMIP6 CMIP abrupt-4xCO2, Earth System Grid Federation, , doi:https://doi.org/10.22033/ESGF/CMIP6.11286, 2020a.

Danabasoglu, G.: NCAR CESM2-FV2 model output prepared for CMIP6 CMIP abrupt-4xCO2, Earth System Grid Federation, , doi:https://doi.org/10.22033/ESGF/CMIP6.11285, 2020b.

Danabasoglu, G., Lawrence, D., Lindsay, K., Lipscomb, W. and Strand, G.: NCAR CESM2 model output prepared for CMIP6 CMIP piControl, Earth System Grid Federation, , doi:https://doi.org/10.22033/ESGF/CMIP6.7733, 2019.

Dix, M., Bi, D., Dobrohotoff, P., Fiedler, R., Harman, I., Law, R., Mackallah, C., Marsland, S., O'Farrell, S., Rashid, H., Srbinovsky, J., Sullivan, A., Trenham, C., Vohralik, P., Watterson, I., Williams, G., Woodhouse, M., Bodman, R., Dias, F. B., Domingues, C., Hannah, N., Heerdegen, A., Savita, A., Wales, S., Allen, C., Druken, K., Evans, B., Richards, C., Ridzwan, S. M., Roberts, D., Smillie, J., Snow, K., Ward, M. and Yang, R.: CSIRO-ARCCSS ACCESS-CM2 model output prepared for CMIP6 CMIP abrupt-4xCO2, Earth System Grid Federation, , doi:https://doi.org/10.22033/ESGF/CMIP6.4237, 2019a.

Dix, M., Bi, D., Dobrohotoff, P., Fiedler, R., Harman, I., Law, R., Mackallah, C., Marsland, S., O'Farrell, S., Rashid, H., Srbinovsky, J., Sullivan, A., Trenham, C., Vohralik, P., Watterson, I., Williams, G., Woodhouse, M., Bodham, R., Dias, F. B., Domingues, C. M., Hannah, N., Heerdegen, A., Savita, A., Wales, S., Allen, C., Druken, K., Evans, B., Richards, C., Ridzwan, S. M., Robers, D., Smillie, J., Snow, K., Ward, M. and Yang, R.: CSIRO-ARCCSS ACCESS-CM2 model output prepared for CMIP6 CMIP historical, Earth System Grid Federation, , doi:https://doi.org/10.22033/ESGF/CMIP6.4271, 2019b.

Dix, M., Bi, D., Dobrohotoff, P., Fiedler, R., Harman, I., Law, R., Mackallah, C., Marsland, S., O'Farrell, S., Rashid, H., Srbinovsky, J., Sullivan, A., Trenham, C., Vohralik, P., Watterson, I., Williams, G., Woodhouse, M., Bodman, R., Dias, F. B., Domingues, C., Hannah, N., Heerdegen, A., Savita, A., Wales, S., Allen, C., Druken, K., Evans, B., Richards, C., Ridzwan, S. M., Roberts, D., Smillie, J., Snow, K., Ward, M. and Yang, R.: CSIRO-ARCCSS ACCESS-CM2 model output prepared for CMIP6 CMIP piControl, Earth System Grid Federation, , doi:https://doi.org/10.22033/ESGF/CMIP6.4311, 2019c.

Dix, M., Bi, D., Dobrohotoff, P., Fiedler, R., Harman, I., Law, R., Mackallah, C., Marsland, S., O'Farrell, S., Rashid, H., Srbinovsky, J., Sullivan, A., Trenham, C., Vohralik, P., Watterson, I., Williams, G., Woodhouse, M., Bodman, R., Dias, F. B., Domingues, C. M., Hannah, N., Heerdegen, A., Savita, A., Wales, S., Allen, C., Druken, K., Evans, B., Richards, C., Ridzwan, S. M., Roberts, D., Smillie, J., Snow, K., Ward, M. and Yang, R.: CSIRO-ARCCSS ACCESS-CM2 model output prepared for CMIP6 ScenarioMIP ssp126, Earth System Grid Federation, , doi:https://doi.org/10.22033/ESGF/CMIP6.4319, 2019d.

Dix, M., Bi, D., Dobrohotoff, P., Fiedler, R., Harman, I., Law, R., Mackallah, C., Marsland, S., O'Farrell, S., Rashid, H., Srbinovsky, J., Sullivan, A., Trenham, C., Vohralik, P., Watterson, I., Williams, G., Woodhouse, M., Bodman, R., Dias, F. B., Domingues, C., Hannah, N., Heerdegen, A., Savita, A., Wales, S., Allen, C., Druken, K., Evans, B., Richards, C., Ridzwan, S. M., Roberts, D., Smillie, J., Snow, K., Ward, M. and Yang, R.: CSIRO-ARCCSS ACCESS-CM2 model output prepared for CMIP6 ScenarioMIP ssp245, Earth System Grid Federation, , doi:https://doi.org/10.22033/ESGF/CMIP6.4321, 2019e.

Dix, M., Bi, D., Dobrohotoff, P., Fiedler, R., Harman, I., Law, R., Mackallah, C., Marsland, S., O'Farrell, S., Rashid, H., Srbinovsky, J., Sullivan, A., Trenham, C., Vohralik, P., Watterson, I., Williams, G., Woodhouse, M., Bodman, R., Dias, F. B., Domingues, C., Hannah, N., Heerdegen, A., Savita, A., Wales, S., Allen, C., Druken, K., Evans, B., Richards, C., Ridzwan, S. M., Roberts, D., Smillie, J., Snow, K., Ward, M. and Yang, R.: CSIRO-ARCCSS ACCESS-CM2 model output prepared for CMIP6 ScenarioMIP ssp370, Earth System Grid Federation, , doi:https://doi.org/10.22033/ESGF/CMIP6.4323, 2019f.

Dix, M., Bi, D., Dobrohotoff, P., Fiedler, R., Harman, I., Law, R., Mackallah, C., Marsland, S., O'Farrell, S., Rashid, H., Srbinovsky, J., Sullivan, A., Trenham, C., Vohralik, P., Watterson, I., Williams, G., Woodhouse, M., Bodman, R., Dias, F. B., Domingues, C., Hannah, N., Heerdegen, A., Savita, A., Wales, S., Allen, C., Druken, K., Evans, B., Richards, C., Ridzwan, S. M., Roberts, D., Smillie, J., Snow, K., Ward, M. and Yang, R.: CSIRO-ARCCSS ACCESS-CM2 model output prepared for CMIP6 ScenarioMIP ssp585, Earth System Grid Federation, , doi:https://doi.org/10.22033/ESGF/CMIP6.4332, 2019g.

EC-Earth Consortium (EC-Earth): EC-Earth-Consortium EC-Earth3-Veg model output prepared for CMIP6 CMIP, Earth System Grid Federation, , doi:https://doi.org/10.22033/ESGF/CMIP6.4706, 2019a.

EC-Earth Consortium (EC-Earth): EC-Earth-Consortium EC-Earth3-Veg model output prepared for CMIP6 CMIP abrupt-4xCO2, Earth System Grid Federation, , doi:https://doi.org/10.22033/ESGF/CMIP6.4524, 2019b.

EC-Earth Consortium (EC-Earth): EC-Earth-Consortium EC-Earth3-Veg model output prepared for CMIP6 CMIP piControl, Earth System Grid Federation, , doi:https://doi.org/10.22033/ESGF/CMIP6.4848, 2019c.

EC-Earth Consortium (EC-Earth): EC-Earth-Consortium EC-Earth3-Veg model output prepared for CMIP6 ScenarioMIP ssp119, Earth System Grid Federation, , doi:https://doi.org/10.22033/ESGF/CMIP6.4872, 2019d.

EC-Earth Consortium (EC-Earth): EC-Earth-Consortium EC-Earth3-Veg model output prepared for CMIP6 ScenarioMIP ssp126, Earth System Grid Federation, , doi:https://doi.org/10.22033/ESGF/CMIP6.4876, 2019e.

EC-Earth Consortium (EC-Earth): EC-Earth-Consortium EC-Earth3-Veg model output prepared for CMIP6 ScenarioMIP ssp245, Earth System Grid Federation, , doi:https://doi.org/10.22033/ESGF/CMIP6.4882, 2019f.

EC-Earth Consortium (EC-Earth): EC-Earth-Consortium EC-Earth3-Veg model output prepared for CMIP6 ScenarioMIP ssp370, Earth System Grid Federation, , doi:https://doi.org/10.22033/ESGF/CMIP6.4886, 2019g.

EC-Earth Consortium (EC-Earth): EC-Earth-Consortium EC-Earth3-Veg model output prepared for CMIP6 ScenarioMIP ssp585, Earth System Grid Federation, , doi:https://doi.org/10.22033/ESGF/CMIP6.4914, 2019h.

EC-Earth Consortium (EC-Earth): EC-Earth-Consortium EC-Earth3 model output prepared for CMIP6 CMIP abrupt-4xCO2, Earth System Grid Federation, , doi:https://doi.org/10.22033/ESGF/CMIP6.4518, 2019i.

EC-Earth Consortium (EC-Earth): EC-Earth-Consortium EC-Earth3 model output prepared for CMIP6 CMIP historical, Earth System Grid Federation, , doi:https://doi.org/10.22033/ESGF/CMIP6.4700, 2019j.

EC-Earth Consortium (EC-Earth): EC-Earth-Consortium EC-Earth3 model output prepared for CMIP6 CMIP piControl, Earth System Grid Federation, , doi:https://doi.org/10.22033/ESGF/CMIP6.4842, 2019k.

EC-Earth Consortium (EC-Earth): EC-Earth-Consortium EC-Earth3 model output prepared for CMIP6 ScenarioMIP ssp126, Earth System Grid Federation, , doi:https://doi.org/10.22033/ESGF/CMIP6.4874, 2019l.

EC-Earth Consortium (EC-Earth): EC-Earth-Consortium EC-Earth3 model output prepared for CMIP6 ScenarioMIP ssp370, Earth System Grid Federation, , doi:https://doi.org/10.22033/ESGF/CMIP6.4884, 2019m.

Good, P.: MOHC HadGEM3-GC31-LL model output prepared for CMIP6 ScenarioMIP ssp245, Earth System Grid Federation, , doi:https://doi.org/10.22033/ESGF/CMIP6.10851, 2019.

Good, P.: MOHC HadGEM3-GC31-LL model output prepared for CMIP6 ScenarioMIP ssp126, Earth System Grid Federation, , doi:https://doi.org/10.22033/ESGF/CMIP6.10849, 2020a.

Good, P.: MOHC HadGEM3-GC31-LL model output prepared for CMIP6 ScenarioMIP ssp585, Earth System Grid Federation, , doi:https://doi.org/10.22033/ESGF/CMIP6.10901, 2020b.

Good, P., Sellar, A., Tang, Y., Rumbold, S., Ellis, R., Kelley, D. and Kuhlbrodt, T.: MOHC UKESM1.0-LL model output prepared for CMIP6 ScenarioMIP ssp119, Earth System Grid Federation, , doi:https://doi.org/10.22033/ESGF/CMIP6.6329, 2019a.

Good, P., Sellar, A., Tang, Y., Rumbold, S., Ellis, R., Kelley, D. and Kuhlbrodt, T.: MOHC UKESM1.0-LL model output prepared for CMIP6 ScenarioMIP ssp126, Earth System Grid Federation, , doi:https://doi.org/10.22033/ESGF/CMIP6.6333, 2019b.

Good, P., Sellar, A., Tang, Y., Rumbold, S., Ellis, R., Kelley, D. and Kuhlbrodt, T.: MOHC UKESM1.0-LL model output prepared for CMIP6 ScenarioMIP ssp245, Earth System Grid Federation, , doi:https://doi.org/10.22033/ESGF/CMIP6.6339, 2019c.

Good, P., Sellar, A., Tang, Y., Rumbold, S., Ellis, R., Kelley, D. and Kuhlbrodt, T.: MOHC UKESM1.0-LL model output prepared for CMIP6 ScenarioMIP ssp370, Earth System Grid Federation, , doi:https://doi.org/10.22033/ESGF/CMIP6.6347, 2019d.

Good, P., Sellar, A., Tang, Y., Rumbold, S., Ellis, R., Kelley, D. and Kuhlbrodt, T.: MOHC UKESM1.0-LL model output prepared for CMIP6 ScenarioMIP ssp434, Earth System Grid Federation, , doi:https://doi.org/10.22033/ESGF/CMIP6.6389, 2019e.

Good, P., Sellar, A., Tang, Y., Rumbold, S., Ellis, R., Kelley, D. and Kuhlbrodt, T.: MOHC UKESM1.0-LL model output prepared for CMIP6 ScenarioMIP ssp585, Earth System Grid Federation, , doi:https://doi.org/10.22033/ESGF/CMIP6.6405, 2019f.

Gregory, J. M., Ingram, W. J., Palmer, M. A., Jones, G. S., Stott, P. A., Thorpe, R. B., Lowe, J. A., Johns, T. C. and Williams, K. D.: A new method for diagnosing radiative forcing and climate sensitivity, Geophys. Res. Lett., 31(3), 2–5, doi:10.1029/2003GL018747, 2004.

Guo, H., John, J. G., Blanton, C., McHugh, C., Nikonov, S., Radhakrishnan, A., Zadeh, N. T., Balaji, V., Durachta, J., Dupuis, C., Menzel, R., Robinson, T., Underwood, S., Vahlenkamp, H., Dunne, K. A., Gauthier, P. P., Ginoux, P., Griffies, S. M., Hallberg, R., Harrison, M., Hurlin, W., Malyshev, S., Naik, V., Paulot, F., Paynter, D. J., Ploshay, J., Schwarzkopf, D. M., Seman, C. J., Shao, A., Silvers, L., Wyman, B., Zeng, Y., Adcroft, A., Dunne, J. P., Held, I. M., Krasting, J. P., Horowitz, L. W., Milly, P. C. ., Shevliakova, E., Winton, M. and Zhao, M.: NOAA-GFDL GFDL-CM4 model output prepared for CMIP6 CMIP abrupt-4xCO2, Earth System Grid Federation, , doi:https://doi.org/10.22033/ESGF/CMIP6.8486, 2018a.

Guo, H., John, J. G., Blanton, C., McHugh, C., Nikonov, S., Radhakrishnan, A., Zadeh, N. T., Balaji, V., Durachta, J., Dupuis, C., Menzel, R., Robinson, T., Underwood, S., Vahlenkamp, H., Dunne, K. A., Gauthier, P. P., Ginoux, P., Griffies, S. M., Hallberg, R. W., Harrison, M., Hurlin, W., Malyshev, S., Naik, V., Paulot, F., Paynter, D. J., Ploshay, J., Schwarzkopf, D. M., Seman, C. J., Shao, A., Silvers, L. G., Wyman, B., Zeng, Y., Adcroft, A. J., Dunne, J. P., Held, I. M., Krasting, J. P., Horowitz, L. W., Milly, P. C. ., Shevliakova, E., Winton, M. and Zhao, M.: NOAA-GFDL GFDL-CM4 model output prepared for CMIP6 CMIP historical, Earth System Grid Federation, , doi:https://doi.org/10.22033/ESGF/CMIP6.8594, 2018b.

Guo, H., John, J. G., Blanton, C., McHugh, C., Nikonov, S., Radhakrishnan, A., Zadeh, N. T., Balaji, V., Durachta, J., Dupuis, C., Menzel, R., Robinson, T., Underwood, S., Vahlenkamp, H., Dunne, K. A., Gauthier, P. P., Ginoux, P., Griffies, S. M., Hallberg, R., Harrison, M., Hurlin, W., Malyshev, S., Naik, V., Paulot, F., Paynter, D. J., Ploshay, J., Rand, K., Schwarzkopf, D. M., Seman, C. J., Shao, A., Silvers, L., Wyman, B., Zeng, Y., Adcroft, A., Dunne, J. P., Held, I. M., Krasting, J. P., Horowitz, L. W., Milly, C., Shevliakova, E., Winton, M., Zhao, M., Yan, X. and Zhang, R.: NOAA-GFDL GFDL-CM4 model output prepared for CMIP6 ScenarioMIP ssp245, Earth System Grid Federation, , doi:https://doi.org/10.22033/ESGF/CMIP6.9263, 2018c.

Guo, H., John, J. G., Blanton, C., McHugh, C., Nikonov, S., Radhakrishnan, A., Zadeh, N. T., Balaji, V., Durachta, J., Dupuis, C., Menzel, R., Robinson, T., Underwood, S., Vahlenkamp, H., Dunne, K. A., Gauthier, P. P., Ginoux, P., Griffies, S. M., Hallberg, R., Harrison, M., Hurlin, W., Malyshev, S., Naik, V., Paulot, F., Paynter, D. J., Ploshay, J., Rand, K., Schwarzkopf, D. M., Seman, C. J., Shao, A., Silvers, L., Wyman, B., Zeng, Y., Adcroft, A., Dunne, J. P., Held, I. M., Krasting, J. P., Horowitz, L. W., Milly, C., Shevliakova, E., Winton, M., Zhao, M., Yan, X. and Zhang, R.: NOAA-GFDL GFDL-CM4 model output prepared for CMIP6 ScenarioMIP ssp585, Earth System Grid Federation, , doi:https://doi.org/10.22033/ESGF/CMIP6.9268, 2018d.

Guo, H., John, J. G., Blanton, C., McHugh, C., Nikonov, S., Radhakrishnan, A., Zadeh, N. T., Balaji, V., Durachta, J., Dupuis, C., Menzel, R., Robinson, T., Underwood, S., Vahlenkamp, H., Dunne, K. A., Gauthier, P. P., Ginoux, P., Griffies, S. M., Hallberg, R., Harrison, M., Hurlin, W., Malyshev, S., Naik, V., Paulot, F., Paynter, D. J., Ploshay, J., Schwarzkopf, D. M., Seman, C. J., Shao, A., Silvers, L., Wyman, B., Zeng, Y., Adcroft, A., Dunne, J. P., Held, I. M., Krasting, J. P., Horowitz, L. W., Milly, P. C. ., Shevliakova, E., Winton, M. and Zhao, M.: NOAA-GFDL GFDL-CM4 piControl model output, Earth System Grid Federation, , doi:https://doi.org/10.22033/ESGF/CMIP6.8666, 2018e.

Hajima, T., Abe, M., Arakawa, O., Suzuki, T., Komuro, Y., Ogura, T., Ogochi, K., Watanabe, M., Yamamoto, A., Tatebe, H., Noguchi, M. A., Ohgaito, R., Ito, A., Yamazaki, D., Ito, A., Takata, K., Watanabe, S., Kawamiya, M. and Tachiiri, K.: MIROC MIROC-ES2L model output prepared for CMIP6 CMIP historical, Earth System Grid Federation, , doi:https://doi.org/10.22033/ESGF/CMIP6.5602, 2019.

Hope, A. P., Canty, T. P., Salawitch, R. J., Tribett, W. R. and Bennett, B. F.: Forecasting Global Warming, in Paris Climate Agreement: Beacon of Hope, pp. 51–114, Springer Climate., 2017.

Huang, W.: THU CIESM model output prepared for CMIP6 CMIP historical, Earth System Grid Federation, , doi:https://doi.org/10.22033/ESGF/CMIP6.7789, 2019a.

Huang, W.: THU CIESM model output prepared for CMIP6 ScenarioMIP ssp126, Earth System Grid Federation, , doi:https://doi.org/10.22033/ESGF/CMIP6.8857, 2019b.

Huang, W.: THU CIESM model output prepared for CMIP6 ScenarioMIP ssp245, Earth System Grid Federation, , doi:https://doi.org/10.22033/ESGF/CMIP6.8858, 2020a.

Huang, W.: THU CIESM model output prepared for CMIP6 ScenarioMIP ssp585, Earth System Grid Federation, , doi:https://doi.org/10.22033/ESGF/CMIP6.8863, 2020b.

Ishii, M., Fukuda, Y., Hirahara, S., Yasui, S., Suzuki, T. and Sato, K.: Accuracy of Global Upper Ocean Heat Content Estimation Expected from Present Observational Data Sets, Sci. Online Lett. Atmos., 13(0), 163–167, doi:10.2151/sola.2017-030, 2017.

John, J. G., Blanton, C., McHugh, C., Nikonov, S., Radhakrishnan, A., Rand, K., Vahlenkamp, H., Zadeh, N. T., Gauthier, P. P., Ginoux, P., Harrison, M., Horowitz, L. W., Malyshev, S., Naik, V., Paynter, D. J., Ploshay, J., Silvers, L. G., Stock, C., Winton, M., Zeng, Y. and Dunne, J. P.: NOAA-GFDL GFDL-ESM4 model output prepared for CMIP6 ScenarioMIP ssp119, Earth System Grid Federation, , doi:https://doi.org/10.22033/ESGF/CMIP6.8683, 2018a.

John, J. G., Blanton, C., McHugh, C., Nikonov, S., Radhakrishnan, A., Rand, K., Vahlenkamp, H., Zadeh, N. T., Gauthier, P. P., Ginoux, P., Harrison, M., Horowitz, L. W., Malyshev, S., Naik, V., Paynter, D. J., Ploshay, J., Silvers, L. G., Stock, C., Winton, M., Zeng, Y. and Dunne, J. P.: NOAA-GFDL GFDL-ESM4 model output prepared for CMIP6 ScenarioMIP ssp126, Earth System Grid Federation, , doi:https://doi.org/10.22033/ESGF/CMIP6.8684, 2018b.

John, J. G., Blanton, C., McHugh, C., Radhakrishnan, A., Rand, K., Vahlenkamp, H., Wilson, C., Zadeh, N. T., Gauthier, P. P., Dunne, J. P., Dussin, R., Horowitz, L. W., Lin, P., Malyshev, S., Naik, V., Ploshay, J., Silvers, L., Stock, C., Winton, M. and Zeng, Y.: NOAA-GFDL GFDL-ESM4 model output prepared for CMIP6 ScenarioMIP ssp245, Earth System Grid Federation, , doi:https://doi.org/10.22033/ESGF/CMIP6.8686, 2018c.

John, J. G., Blanton, C., McHugh, C., Nikonov, S., Radhakrishnan, A., Rand, K., Vahlenkamp, H., Zadeh, N. T., Gauthier, P. P., Ginoux, P., Harrison, M., Horowitz, L. W., Malyshev, S., Naik, V., Paynter, D. J., Ploshay, J., Silvers, L., Stock, C., Winton, M., Zeng, Y. and Dunne, J. P.: NOAA-GFDL GFDL-ESM4 model output prepared for CMIP6 ScenarioMIP ssp370, Earth System Grid Federation, , doi:https://doi.org/10.22033/ESGF/CMIP6.8691, 2018d.

John, J. G., Blanton, C., McHugh, C., Nikonov, S., Radhakrishnan, A., Rand, K., Vahlenkamp, H., Zadeh, N. T., Gauthier, P. P., Ginoux, P., Harrison, M., Horowitz, L. W., Malyshev, S., Naik, V., Paynter, D. J., Ploshay, J., Silvers, L., Stock, C., Winton, M., Zeng, Y. and Dunne, J. P.: NOAA-GFDL GFDL-ESM4 model output prepared for CMIP6 ScenarioMIP ssp585, Earth System Grid Federation, , doi:https://doi.org/10.22033/ESGF/CMIP6.8706, 2018e.

Jungclaus, J. H., Bittner, M., Wieners, K.-H., Wachsmann, F., Schupfner, M., Legutke, S., Giorgetta, M., Reick, C., Gayler, V., Haak, H., de Vrese, P., Raddatz, T., Esch, M., Mauritsen, T., von Storch, J.-S., Behrens, J., Brovkin, V., Claussen, M., Crueger, T., Fast, I., Fiedler, S., Hagemann, S., Hohenegger, C., Jahns, T., Kloster, S., Kinne, S., Lasslop, G., Kornblueh, L., Marotzke, J., Matai, D., Meraner, K., Mikolajewicz, U., Modali, K., Muller, W., Nabel, J., Notz, D., Peters, K., Pincus, R., Pohlmann, H., Pongratz, J., Rast, S., Schmidt, H., Schnur, R., Schulzweida, U., Six, K., Stevens, B., Voigt, A. and Roeckner, E.: MPI-M MPI-ESM1.2-HR model output prepared for CMIP6 CMIP historical, Earth System Grid Federation, , doi:https://doi.org/10.22033/ESGF/CMIP6.6594, 2019.

Kelley, M., Schmidt, G., Nazarenko, L., Bauer, S., Ruedy, R., Russell, G., Ackerman, A., Aleinov, I., Bauer, M., Bleck, R., Canuto, V., Cesana, G., Cheng, Y., Clune, T., Cook, B., Cruz, C., Del Genio, A., Elsaesser, G., Faluvegi, G., Kiang, N., Kim, D., Lacis, A., Leboissetier, A., LeGrande, A., Lo, K., Marshall, J., Matthews, E., McDermid, S., Mezuman, K., Miller, R., Murray, L., Oinas, V., Orbe, C., Pérez García-Pando, C., Perlwitz, J., Puma, M., Rind, D., Romanou, A., Shindell, D., Sun, S., Tausnev, N., Tsigaridis, K., Tselioudis, G., Weng, E., Wu, J. and Yao, M.: GISS-E2.1: Configurations and Climatology, J. Adv. Model. Earth Syst., 2018(Phase 6), doi:10.1029/2019MS002025, 2020.

Krasting, J. P., John, J. G., Blanton, C., McHugh, C., Nikonov, S., Radhakrishnan, A., Rand, K., Zadeh, N. T., Balaji, V., Durachta, J., Dupuis, C., Menzel, R., Robinson, T., Underwood, S., Vahlenkamp, H., Dunne, K. A., Gauthier, P. P., Ginoux, P., Griffies, S. M., Hallberg, R., Harrison, M., Hurlin, W., Malyshev, S., Naik, V., Paulot, F., Paynter, D. J., Ploshay, J., Schwarzkopf, D. M., Seman, C. J., Silvers, L., Wyman, B., Zeng, Y., Adcroft, A., Dunne, J. P., Guo, H., Held, I. M., Horowitz, L. W., Milly, P. C. ., Shevliakova, E., Stock, C., Winton, M. and Zhao, M.: NOAA-GFDL GFDL-ESM4 model output prepared for CMIP6 CMIP abrupt-4xCO2, Earth System Grid Federation, , doi:https://doi.org/10.22033/ESGF/CMIP6.8489, 2018a.

Krasting, J. P., John, J. G., Blanton, C., McHugh, C., Nikonov, S., Radhakrishnan, A., Rand, K., Zadeh, N. T., Balaji, V., Durachta, J., Dupuis, C., Menzel, R., Robinson, T., Underwood, S., Vahlenkamp, H., Dunne, K. A., Gauthier, P. P., Ginoux, P., Griffies, S. M., Hallberg, R. W., Harrison, M., Hurlin, W., Malyshev, S., Naik, V., Paulot, F., Paynter, D. J., Ploshay, J., Schwarzkopf, D. M., Seman, C. J., Silvers, L. G., Wyman, B., Zeng, Y., Adcroft, A. J., Dunne, J. P., Guo, H., Held, I. M., Horowitz, L. W., Milly, P. C. ., Shevliakova, E., Stock, C., Winton, M. and Zhao, M.: NOAA-GFDL GFDL-ESM4 model output prepared for CMIP6 CMIP historical, Earth System Grid Federation, , doi:https://doi.org/10.22033/ESGF/CMIP6.8597, 2018b.

Krasting, J. P., John, J. G., Blanton, C., McHugh, C., Nikonov, S., Radhakrishnan, A., Rand, K., Zadeh, N. T., Balaji, V., Durachta, J., Dupuis, C., Menzel, R., Robinson, T., Underwood, S., Vahlenkamp, H., Dunne, K. A., Gauthier, P. P., Ginoux, P., Griffies, S. M., Hallberg, R., Harrison, M., Hurlin, W., Malyshev, S., Naik, V., Paulot, F., Paynter, D. J., Ploshay, J., Schwarzkopf, D. M., Seman, C. J., Silvers, L., Wyman, B., Zeng, Y., Adcroft, A., Dunne, J. P., Guo, H., Held, I. M., Horowitz, L. W., Milly, P. C. ., Shevliakova, E., Stock, C., Winton, M. and Zhao, M.: NOAA-GFDL GFDL-ESM4 model output prepared for CMIP6 CMIP piControl, Earth System Grid Federation, , doi:https://doi.org/10.22033/ESGF/CMIP6.8669, 2018c.

Levitus, S., Antonov, J. I., Boyer, T. P., Baranova, O. K., Garcia, H. E., Locarnini, R. A., Mishonov, A. V., Reagan, J. R., Seidov, D., Yarosh, E. S. and Zweng, M. M.: World ocean heat content and thermosteric sea level change (0-2000m), 1955-2010, Geophys. Res. Lett., 39(10), 1–5, doi:10.1029/2012GL051106, 2012.

Li, L.: CAS FGOALS-g3 model output prepared for CMIP6 CMIP historical, Earth System Grid Federation, , doi:https://doi.org/10.22033/ESGF/CMIP6.3356, 2019a.

Li, L.: CAS FGOALS-g3 model output prepared for CMIP6 ScenarioMIP ssp126, Earth System Grid Federation, , doi:https://doi.org/10.22033/ESGF/CMIP6.3465, 2019b.

Li, L.: CAS FGOALS-g3 model output prepared for CMIP6 ScenarioMIP ssp245, Earth System Grid Federation, , doi:https://doi.org/10.22033/ESGF/CMIP6.3469, 2019c.

Li, L.: CAS FGOALS-g3 model output prepared for CMIP6 ScenarioMIP ssp370, Earth System Grid Federation, , doi:https://doi.org/10.22033/ESGF/CMIP6.3480, 2019d.

Li, L.: CAS FGOALS-g3 model output prepared for CMIP6 ScenarioMIP ssp585, Earth System Grid Federation, , doi:https://doi.org/10.22033/ESGF/CMIP6.3503, 2019e.

Meinshausen, M., Smith, S. J., Calvin, K., Daniel, J. S., Kainuma, M. L. T., Lamarque, J., Matsumoto, K., Montzka, S. A., Raper, S. C. B., Riahi, K., Thomson, A., Velders, G. J. M. and van Vuuren, D. P. P.: The RCP greenhouse gas concentrations and their extensions from 1765 to 2300, Clim. Change, 109(1), 213–241, doi:10.1007/s10584-011-0156-z, 2011.

Myhre, G., Shindell, D., Bréon, F.-M., Collins, W., Fuglestvedt, J., Huang, J., Koch, D., Lamarque, J.-F., Lee, D., Mendoza, B., Nakajima, T., Robock, A., Stephens, G., Takemura, T. and Zhang, H.: Anthropogenic and Natural Radiative Forcing, Clim. Chang. 2013 Phys. Sci. Basis. Contrib. Work. Gr. I to Fifth Assess. Rep. Intergov. Panel Clim. Chang., 659–740, doi:10.1017/ CBO9781107415324.018, 2013.

NASA Goddard Institute for Space Studies (NASA/GISS): NASA-GISS GISS-E2.1G model output prepared for CMIP6 CMIP abrupt-4xCO2, Earth System Grid Federation, , doi:https://doi.org/10.22033/ESGF/CMIP6.6976, 2018a.

NASA Goddard Institute for Space Studies (NASA/GISS): NASA-GISS GISS-E2.1G model output prepared for CMIP6 CMIP historical, Earth System Grid Federation, , doi:https://doi.org/10.22033/ESGF/CMIP6.7127, 2018b.

NASA Goddard Institute for Space Studies (NASA/GISS): NASA-GISS GISS-E2.1G model output prepared for CMIP6 CMIP piControl, Earth System Grid Federation, , doi:https://doi.org/10.22033/ESGF/CMIP6.7380, 2018c.

NASA Goddard Institute for Space Studies (NASA/GISS): NASA-GISS GISS-E2.1H model output prepared for CMIP6 CMIP piControl, Earth System Grid Federation, , doi:https://doi.org/10.22033/ESGF/CMIP6.7381, 2018d.

NASA Goddard Institute for Space Studies (NASA/GISS): NASA-GISS GISS-E2-2-G model output prepared for CMIP6 CMIP abrupt-4xCO2, Earth System Grid Federation, , doi:https://doi.org/10.22033/ESGF/CMIP6.6978, 2019a.

NASA Goddard Institute for Space Studies (NASA/GISS): NASA-GISS GISS-E2.1H model output prepared for CMIP6 CMIP abrupt-4xCO2, Earth System Grid Federation, , doi:https://doi.org/10.22033/ESGF/CMIP6.6977, 2019b.

NASA Goddard Institute for Space Studies (NASA/GISS): NASA-GISS GISS-E2.1H model output prepared for CMIP6 CMIP historical, Earth System Grid Federation, , doi:https://doi.org/10.22033/ESGF/CMIP6.7128, 2019c.

NASA Goddard Institute for Space Studies (NASA/GISS): NASA-GISS GISS-E2.1G model output prepared for CMIP6 ScenarioMIP ssp126, Earth System Grid Federation, , doi:https://doi.org/10.22033/ESGF/CMIP6.7410, 2020a.

NASA Goddard Institute for Space Studies (NASA/GISS): NASA-GISS GISS-E2.1G model output prepared for CMIP6 ScenarioMIP ssp245, Earth System Grid Federation, , doi:https://doi.org/10.22033/ESGF/CMIP6.7415, 2020b.

NASA Goddard Institute for Space Studies (NASA/GISS): NASA-GISS GISS-E2.1G model output prepared for CMIP6 ScenarioMIP ssp370, Earth System Grid Federation, , doi:https://doi.org/10.22033/ESGF/CMIP6.7426, 2020c.

NASA Goddard Institute for Space Studies (NASA/GISS): NASA-GISS GISS-E2.1G model output prepared for CMIP6 ScenarioMIP ssp585, Earth System Grid Federation, , doi:https://doi.org/10.22033/ESGF/CMIP6.7460, 2020d.

Neubauer, D., Ferrachat, S., Siegenthaler-Le Drian, C., Stoll, J., Folini, D. S., Tegen, I., Wieners, K.-H., Mauritsen, T., Stemmler, I., Barthel, S., Bey, I., Daskalakis, M., Heinold, B., Kokkola, H., Partridge, D., Rast, S., Schmidt, H., Schutgens, N., Stanelle, T., Stier, P., Watson-Parrs, D. and Lohmann, U.: HAMMOZ-Consortium MPI-ESM1.2-HAM model output prepared for CMIP6 CMIP6 historical, Earth System Grid Federation, , doi:https://doi.org/10.22033/ESGF/CMIP6.5016, 2019.

Park, S. and Shin, J.: SNU SAM0-UNICON model output prepared for CMIP6 CMIP abrupt-4xCO2, Earth System Grid Federation, , doi:https://doi.org/10.22033/ESGF/CMIP6.7783, 2019a.

Park, S. and Shin, J.: SNU SAM0-UNICON model output prepared for CMIP6 CMIP historical, Earth System Grid Federation, , doi:https://doi.org/10.22033/ESGF/CMIP6.7789, 2019b.

Park, S. and Shin, J.: SNU SAM0-UNICON model output prepared for CMIP6 CMIP piControl, Earth System Grid Federation, , doi:https://doi.org/10.22033/ESGF/CMIP6.7791, 2019c.

Ridley, J., Menary, M., Kuhlbrodt, T., Andrews, M. and Andrews, T.: MOHC HadGEM3-GC31-LL model output prepared for CMIP6 CMIP piControl, Earth System Grid Federation, , doi:https://doi.org/10.22033/ESGF/CMIP6.6294, 2018.

Ridley, J., Menary, M., Kuhlbrodt, T., Andrews, M. and Andrews, T.: MOHC HadGEM3-GC31-LL model output prepared for CMIP6 CMIP, Earth System Grid Federation, , doi:https://doi.org/10.22033/ESGF/CMIP6.6109, 2019a.

Ridley, J., Menary, M., Kuhlbrodt, T., Andrews, M. and Andrews, T.: MOHC HadGEM3-GC31-LL model output prepared for CMIP6 CMIP abrupt-4xCO2, Earth System Grid Federation, , doi:https://doi.org/10.22033/ESGF/CMIP6.5839, 2019b.

Ridley, J., Menary, M., Kuhlbrodt, T., Andrews, M. and Andrews, T.: MOHC HadGEM3-GC31-MM model output prepared for CMIP6 CMIP historical, Earth System Grid Federation, , doi:https://doi.org/10.22033/ESGF/CMIP6.6112, 2019c.

Rong, X.: CAMS CAMS_CSM1.0 model output preapred for CMIP6 CMIP historical, Earth System Grid Federation, , doi:https://doi.org/10.22033/ESGF/CMIP6.9754, 2019a.

Rong, X.: CAMS CAMS-CSM1.0 model output prepared for CMIP6 ScenarioMIP ssp119, Earth System Grid Federation, , doi:https://doi.org/10.22033/ESGF/CMIP6.11045, 2019b.

Rong, X.: CAMS CAMS-CSM1.0 model output prepared for CMIP6 ScenarioMIP ssp126, Earth System Grid Federation, , doi:https://doi.org/10.22033/ESGF/CMIP6.11046, 2019c.

Rong, X.: CAMS CAMS-CSM1.0 model output prepared for CMIP6 ScenarioMIP ssp245, Earth System Grid Federation, , doi:https://doi.org/10.22033/ESGF/CMIP6.11047, 2019d.

Rong, X.: CAMS CAMS-CSM1.0 model output prepared for CMIP6 ScenarioMIP ssp370, Earth System Grid Federation, , doi:https://doi.org/10.22033/ESGF/CMIP6.11048, 2019e.

Rong, X.: CAMS CAMS-CSM1.0 model output prepared for CMIP6 ScenarioMIP ssp585, Earth System Grid Federation, , doi:https://doi.org/10.22033/ESGF/CMIP6.11052, 2019f.

Schupfner, M., Wieners, K.-H., Wachsmann, F., Steger, C., Bittner, M., Jungclaus, J., Früh, B., Pankatz, K., Giorgetta, M., Reick, C., Legutke, S., Esch, M., Gayler, V., Haak, H., de Vrese, P., Raddatz, T., Mauritsen, T., von Storch, J.-S., Behrens, J., Brovkin, V., Claussen, M., Crueger, T., Fast, I., Fiedler, S., Hagemann, S., Hohenegger, C., Jahns, T., Kloster, S., Kinne, S., Lasslop, G., Kornblueh, L., Marotzke, J., Matei, D., Meraner, K., Mikolajewicz, U., Modali, K., Müller, W., Nabel, J., Notz, D., Peters, K., Pincus, R., Pohlmann, H., Pongratz, J., Rast, S., Schmidt, H., Schnur, R., Schulzweida, U., Six, K., Stevens, B., Voigt, A. and Roeckner, E.: DKRZ MIP-ESM1.2-HR model output prepared for CMIP6 ScenarioMIP ssp126, Earth System Grid Federation, , doi:https://doi.org/10.22033/ESGF/CMIP6.4397, 2019a.

Schupfner, M., Wieners, K.-H., Wachsmann, F., Steger, C., Bittner, M., Jungclaus, J., Früh, B., Pankatz, K., Giorgetta, M., Reick, C., Legutke, S., Esch, M., Gayler, V., Haak, H., de Vrese, P., Raddatz, T., Mauritsen, T., von Storch, J.-S., Behrens, J., Brovkin, V., Claussen, M., Crueger, T., Fast, I., Fiedler, S., Hagemann, S., Hohenegger, C., Jahns, T., Kloster, S., Kinne, S., Lasslop, G., Kornblueh, L., Marotzke, J., Matei, D., Meraner, K., Mikolajewicz, U., Modali, K., Müller, W., Nabel, J., Notz, D., Peters, K., Pincus, R., Pohlmann, H., Pongratz, J., Rast, S., Schmidt, H., Schnur, R., Schulzweida, U., Six, K., Stevens, B., Voigt, A. and Roeckner, E.: DKRZ MPI-ESM1.2-HR model output prepared for CMIP6 ScenarioMIP ssp245, Earth System Grid Federation, , doi:https://doi.org/10.22033/ESGF/CMIP6.4398, 2019b.

Schupfner, M., Wieners, K.-H., Wachsmann, F., Steger, C., Bittner, M., Jungclaus, J., Früh, B., Pankatz, K., Giorgetta, M., Reick, C., Legutke, S., Esch, M., Gayler, V., Haak, H., de Vrese, P., Raddatz, T., Mauritsen, T., von Storch, J.-S., Behrens, J., Brovkin, V., Claussen, M., Crueger, T., Fast, I., Fiedler, S., Hagemann, S., Hohenegger, C., Jahns, T., Kloster, S., Kinne, S., Lasslop, G., Kornblueh, L., Marotzke, J., Matei, D., Meraner, K., Mikolajewicz, U., Modali, K., Müller, W., Nabel, J., Notz, D., Peters, K., Pincus, R., Pohlmann, H., Pongratz, J., Rast, S., Schmidt, H., Schnur, R., Schulzweida, U., Six, K., Stevens, B., Voigt, A. and Roeckner, E.: DKRZ MPI-ESM1.2-HR model output prepared for CMIP6 ScenarioMIP ssp370, Earth System Grid Federation, , doi:https://doi.org/10.22033/ESGF/CMIP6.4399, 2019c.

Schupfner, M., Wieners, K.-H., Wachsmann, F., Steger, C., Bittner, M., Jungclaus, J., Früh, B., Pankatz, K., Giorgetta, M., Reick, C., Legutke, S., Esch, M., Gayler, V., Haak, H., de Vrese, P., Raddatz, T., Mauritsen, T., von Storch, J.-S., Behrens, J., Brovkin, V., Claussen, M., Crueger, T., Fast, I., Fiedler, S., Hagemann, S., Hohenegger, C., Jahns, T., Kloster, S., Kinne, S., Lasslop, G., Kornblueh, L., Marotzke, J., Matei, D., Meraner, K., Mikolajewicz, U., Modali, K., Müller, W., Nabel, J., Notz, D., Peters, K., Pincus, R., Pohlmann, H., Pongratz, J., Rast, S., Schmidt, H., Schnur, R., Schulzweida, U., Six, K., Stevens, B., Voigt, A. and

Roeckner, E.: DKRZ MPI-ESM1.2-HR model output prepared for CMIP6 ScenarioMIP ssp585, Earth System Grid Federation, , doi:https://doi.org/10.22033/ESGF/CMIP6.4403, 2019d.

Schwartz, S. E.: Determination of Earth's Transient and Equilibrium Climate Sensitivities from Observations Over the Twentieth Century: Strong Dependence on Assumed Forcing, Surv. Geophys., 33(3–4), 745–777, doi:10.1007/s10712-012-9180-4, 2012.

Seferian, R.: CNRM-CERFACS CNRM-ESM2-1 model output prepared for CMIP6 CMIP historical, Earth System Grid Federation, , doi:https://doi.org/10.22033/ESGF/CMIP6.4068, 2018.

Seland, Ø., Bentsen, M., Oliviè, D. J. L., Toniazzo, T., Gjermundsen, A., Graff, L. S., Debernard, J. B., Gupta, A. K., He, Y., Kirkevåg, A., Schwinger, J., Tjiputra, J., Aas, K. S., Bethke, I., Fan, Y., Griesfeller, J., Grini, A., Guo, C., Ilicak, M., Karset, I. H. H., Landgren, O. A., Liakka, J., Moseid, K. O., Nummelin, A., Spensberger, C., Tang, H., Zhang, Z., Heinze, C., Iversen, T. and Schulz, M.: NCC NorESM2-LM model output prepared for CMIP6 CMIP abrupt-4xCO2, Earth System Grid Federation, , doi:https://doi.org/10.22033/ESGF/CMIP6.7836, 2019a.

Seland, Ø., Bentsen, M., Oliviè, D. J. L., Toniazzo, T., Gjermundsen, A., Graff, L. S., Debernard, J. B., Gupta, A. K., He, Y., Kirkevåg, A., Schwinger, J., Tjiputra, J., Aas, K. S., Bethke, I., Fan, Y., Griesfeller, J., Grini, A., Guo, C., Ilicak, M., Karset, I. H. H., Landgren, O. A., Liakka, J., Moseid, K. O., Nummelin, A., Spensberger, C., Tang, H., Zhang, Z., Heinze, C., Iversen, T. and Schulz, M.: NCC NorESM2-LM model output prepared for CMIP6 CMIP piControl, Earth System Grid Federation, , doi:https://doi.org/10.22033/ESGF/CMIP6.8217, 2019b.

Seland, Ø., Bentsen, M., Oliviè, D. J. L., Toniazzo, T., Gjermundsen, A., Graff, L. S., Debernard, J. B., Gupta, A. K., He, Y., Kirkevåg, A., Schwinger, J., Tjiputra, J., Aas, K. S., Bethke, I., Fan, Y., Griesfeller, J., Grini, A., Guo, C., Ilicak, M., Karset, I. H. H., Landgren, O. A., Liakka, J., Moseid, K. O., Nummelin, A., Spensberger, C., Tang, H., Zhang, Z., Heinze, C., Iversen, T. and Schulz, M.: NCC NorESM2-LM model output prepared for CMIP6 ScenarioMIP ssp126, Earth System Grid Federation, , doi:https://doi.org/10.22033/ESGF/CMIP6.8248, 2019c.

Seland, Ø., Bentsen, M., Oliviè, D. J. L., Toniazzo, T., Gjermundsen, A., Graff, L. S., Debernard, J. B., Gupta, A. K., He, Y., Kirkevåg, A., Schwinger, J., Tjiputra, J., Aas, K. S., Bethke, I., Fan, Y., Griesfeller, J., Grini, A., Guo, C., Ilicak, M., Karset, I. H. H., Landgren, O. A., Liakka, J., Moseid, K. O., Nummelin, A., Spensberger, C., Tang, H., Zhang, Z., Heinze, C., Iversen, T. and Schulz, M.: NCC NorESM2-LM model output prepared for CMIP6 ScenarioMIP ssp245, Earth System Grid Federation, , doi:https://doi.org/10.22033/ESGF/CMIP6.8253, 2019d.

Seland, Ø., Bentsen, M., Oliviè, D. J. L., Toniazzo, T., Gjermundsen, A., Graff, L. S., Debernard, J. B., Gupta, A. K., He, Y., Kirkevåg, A., Schwinger, J., Tjiputra, J., Aas, K. S., Bethke, I., Fan, Y., Griesfeller, J., Grini, A., Guo, C., Ilicak, M., Karset, I. H. H., Landgren, O. A., Liakka, J., Moseid, K. O., Nummelin, A., Spensberger, C., Tang, H., Zhang, Z., Heinze, C., Iversen, T. and Schulz, M.: NCC NorESM2-LM model output prepared for CMIP6 ScenarioMIP ssp370, Earth System Grid Federation, , doi:https://doi.org/10.22033/ESGF/CMIP6.8268, 2019e.

Seland, Ø., Bentsen, M., Oliviè, D. J. L., Toniazzo, T., Gjermundsen, A., Graff, L. S., Debernard, J. B., Gupta, A. K., He, Y., Kirkevåg, A., Schwinger, J., Tjiputra, J., Aas, K. S., Bethke, I., Fan, Y., Griesfeller, J., Grini, A., Guo, C., Ilicak, M., Karset, I. H. H., Landgren, O. A., Liakka, J., Moseid, K. O., Nummelin, A., Spensberger, C., Tang, H., Zhang, Z., Heinze, C., Iversen, T. and Schulz, M.: NCC NorESM2-LM model output prepared for CMIP6 ScenarioMIP ssp585, Earth System Grid Federation, , doi:https://doi.org/10.22033/ESGF/CMIP6.8319, 2019f.

Seland, Ø., Bentsen, M., Oliviè, D. J. L., Toniazzo, T., Gjermundsen, A., Graff, L. S., Debernard, J. B., Gupta, A. K., He, Y., Kirkevåg, A., Schwinger, J., Tjiputra, J., Aas, K. S., Bethke, I., Fan, Y., Griesfeller, J., Grini, A., Guo, C., Ilicak, M., Karset, I. H. H., Landgren, O. A., Liakka, J., Moseid, K. O., Nummelin, A., Spensberger, C., Tang, H., Zhang, Z., Heinze, C., Iversen, T. and Schulz, M.: NCC NorESM2-LM output prepared for CMIP6 CMIP historical, Earth System Grid Federation, , doi:https://doi.org/10.22033/ESGF/CMIP6.8036, 2019g.

Semmler, T., Danilov, S., Rackow, T., Sidorenko, D., Barbi, D., Hegewald, J., Sein, D., Wang, Q. and Jung, T.: AWI AWI-CM1.1MR model output prepared for CMIP6 CMIP historical, Earth System Grid Federation, , doi:https://doi.org/10.22033/ESGF/CMIP6.2686, 2018a.

Semmler, T., Danilov, S., Rackow, T., Sidorenko, D., Barbi, D., Hegewald, J., Pradhan, H. K., Sein, D., Wang, Q. and Jung, T.: AWI AWI-CM1.1MR model output prepared for CMIP6 ScenarioMIP ssp126, Earth System Grid Federation, , doi:https://doi.org/10.22033/ESGF/CMIP6.2796, 2018b.

Semmler, T., Danilov, S., Rackow, T., Sidorenko, D., Barbi, D., Hegewald, J., Pradhan, H. K., Sein, D., Wang, Q. and Jung, T.: AWI AWI-CM1.1MR model output prepared for CMIP6 ScenarioMIP ssp246, Earth System Grid Federation, , doi:https://doi.org/10.22033/ESGF/CMIP6.2800, 2018c.

Semmler, T., Danilov, S., Rackow, T., Sidorenko, D., Barbi, D., Hegewald, J., Pradhan, H. K., Sein, D., Wang, Q. and Jung, T.: AWI AWI-CM1.1MR model output prepared for CMIP6 ScenarioMIP ssp370, Earth System Grid Federation, , doi:https://doi.org/10.22033/ESGF/CMIP6.2803, 2019a.

Semmler, T., Danilov, S., Rackow, T., Sidorenko, D., Barbi, D., Hegewald, J., Pradhan, H. K., Sein, D., Wang, Q. and Jung, T.: AWI AWI-CM1.1MR model output prepared for CMIP6 ScenarioMIP ssp585, Earth System Grid Federation, , doi:https://doi.org/10.22033/ESGF/CMIP6.2817, 2019b.

Shiogama, H., Abe, M. and Tatebe, H.: MIROC MIROC6 model output prepared for CMIP6 ScenarioMIP ssp119, Earth System Grid Federation, , doi:https://doi.org/10.22033/ESGF/CMIP6.5741, 2019a.

Shiogama, H., Abe, M. and Tatebe, H.: MIROC MIROC6 model output prepared for CMIP6 ScenarioMIP ssp126, Earth System Grid Federation, , doi:https://doi.org/10.22033/ESGF/CMIP6.5743, 2019b.

Shiogama, H., Abe, M. and Tatebe, H.: MIROC MIROC6 model output prepared for CMIP6 ScenarioMIP ssp245, Earth System Grid Federation, , doi:https://doi.org/10.22033/ESGF/CMIP6.5746, 2019c.

Shiogama, H., Abe, M. and Tatebe, H.: MIROC MIROC6 model output prepared for CMIP6 ScenarioMIP ssp370, Earth System Grid Federation, , doi:https://doi.org/10.22033/ESGF/CMIP6.5752, 2019d.

Shiogama, H., Abe, M. and Tatebe, H.: MIROC MIROC6 model output prepared for CMIP6 ScenarioMIP ssp434, Earth System Grid Federation, , doi:https://doi.org/10.22033/ESGF/CMIP6.5764, 2019e.

Shiogama, H., Abe, M. and Tatebe, H.: MIROC MIROC6 model output prepared for CMIP6 ScenarioMIP ssp460, Earth System Grid Federation, , doi:https://doi.org/10.22033/ESGF/CMIP6.5766, 2019f.

Shiogama, H., Abe, M. and Tatebe, H.: MIROC MIROC6 model output prepared for CMIP6 ScenarioMIP ssp585, Earth System Grid Federation, , doi:https://doi.org/10.22033/ESGF/CMIP6.5771, 2019g.

Song, Z., Qiao, F., Bao, Y., Shu, Q., Song, Y. and Yang, X.: FIO-QLNM FIO-ESM2.0 model output prepared for CMIP6 CMIP historical, Earth System Grid Federation, , doi:https://doi.org/10.22033/ESGF/CMIP6.9199, 2019a.

Song, Z., Qiao, F., Bao, Y., Shu, Q., Song, Y. and Yang, X.: FIO-QLNM FIO-ESM2.0 model output prepared for CMIP6 ScenarioMIP ssp126, Earth System Grid Federation, , doi:https://doi.org/10.22033/ESGF/CMIP6.9208, 2019b.

Song, Z., Qiao, F., Bao, Y., Shu, Q., Song, Y. and Yang, X.: FIO-QLNM FIO-ESM2.0 model output prepared for CMIP6 ScenarioMIP ssp245, Earth System Grid Federation, , doi:https://doi.org/10.22033/ESGF/CMIP6.9209, 2019c.

Song, Z., Qiao, F., Bao, Y., Shu, Q., Song, Y. and Yang, X.: FIO-QLNM FIO-ESM2.0 model output prepared for CMIP6 ScenarioMIP ssp585, Earth System Grid Federation, , doi:https://doi.org/10.22033/ESGF/CMIP6.9214, 2019d.

Steger, C., Schupfner, M., Wieners, K.-H., Wachsmann, F., Bittner, M., Jungclaus, J., Früh, B., Pankatz, K., Giorgetta, M., Reick, C., Legutke, S., Esch, M., Gayler, V., Haak, H., de Vrese, P., Raddatz, T., Mauritsen, T., von Storch, J.-S., Behrens, J., Brovkin, V., Claussen, M., Crueger, T., Fast, I., Fiedler, S., Hagemann, S., Hohenegger, C., Jahns, T., Kloster, S., Kinne, S., Lasslop, G., Kornblueh, L., Marotzke, J., Matei, D., Meraner, K., Mikolajewicz, U., Modali, K., Müller, W., Nabel, J., Notz, D., Peters, K., Pincus, R., Pohlmann, H., Pongratz, J., Rast, S., Schmidt, H., Schnur, R., Schulzweida, U., Ix, K., Stevens, B., Voigt, A. and Roeckner, E.: DWD MPI-ESM1.2-HR model output prepared for CMIP6 ScenarioMIP ssp585, Earth System Grid Federation, , doi:https://doi.org/10.22033/ESGF/CMIP6.4479, 2019.

Stouffer, R. J.: UA MCM-UA-1-0 model output prepared for CMIP6 CMIP abrupt-4xCO2, Earth System Grid Federation, , doi:https://doi.org/10.22033/ESGF/CMIP6.8882, 2019a.

Stouffer, R. J.: UA MCM-UA-1-0 model output prepared for CMIP6 CMIP historical, Earth System Grid Federation, , doi:https://doi.org/10.22033/ESGF/CMIP6.8888, 2019b.

Stouffer, R. J.: UA MCM-UA-1-0 model output prepared for CMIP6 CMIP piControl, Earth System Grid Federation, , doi:https://doi.org/10.22033/ESGF/CMIP6.8890, 2019c.

Stouffer, R. J.: UA MCM-UA-1-0 model output prepared for CMIP6 ScenarioMIP ssp245, Earth System Grid Federation, , doi:https://doi.org/10.22033/ESGF/CMIP6.13896, 2019d.

Stouffer, R. J.: UA MCM-UA-1-0 model output prepared for CMIP6 ScenarioMIP ssp370, Earth System Grid Federation, , doi:https://doi.org/10.22033/ESGF/CMIP6.13897, 2019e.

Stouffer, R. J.: UA MCM-UA-1-0 model output prepared for CMIP6 ScenarioMIP ssp585, Earth System Grid Federation, , doi:https://doi.org/10.22033/ESGF/CMIP6.13901, 2019f.

Stouffer, R. J.: UA MCM-UA-1.0 model output prepared for CMIP6 ScenarioMIP ssp126, Earth System Grid Federation, , doi:https://doi.org/10.22033/ESGF/CMIP6.13895, 2019g.

Swart, N. C., Jason, N. ., Kharin, V. V., Lazare, M., Scinocca, J. F., Gillett, N. P., Anstey, J., Arora, V. K., Christian, J. R., Jiao, Y., Lee, W. G., Majaess, F., Saenko, O. A., Seiler, C., Seinen, C., Shao, A., Solheim, L., von Salzen, K., Yang, D., Winter, B. and Sigmond, M.: CCCma CanESM5-CanOE model output prepared for CMIP6 CMIP, Earth System Grid Federation, , doi:https://doi.org/10.22033/ESGF/CMIP6.10260, 2019a.

Swart, N. C., Cole, J. N. S., Kharin, V. V., Lazare, M., Scinocca, J. F., Gillett, N. P., Anstey, J., Arora, V. K., Christian, J. R., Jiao, Y., Lee, W. G., Majaess, F., Saenko, O. A., Seiler, C., Seinen, C., Shao, A., Solheim, L., von Salzen, K., Yang, D., Winter, B. and Sigmond, M.: CCCma CaneSM5-CanOE model output prepared for CMIP6 ScenarioMIP ssp126, Earth System Grid Federation, , doi:https://doi.org/10.22033/ESGF/CMIP6.10269, 2019b.

Swart, N. C., Cole, J. N. S., Kharin, V. V., Lazare, M., Scinocca, J. F., Gillett, N. P., Anstey, J., Arora, V., Christian, J. R., Jiao, Y., Lee, W. G., Majaess, F., Saenko, O. A., Seiler, C., Seinen, C., Shao, A., Solheim, L., von Salzen, K., Yang, D., Winter, B. and Sigmond, M.: CCCma CanESM5-CanOE model output prepared for CMIP6 ScenarioMIP ssp245, Earth System Grid Federation, , doi:https://doi.org/10.22033/ESGF/CMIP6.10270, 2019c.

Swart, N. C., Cole, J. N. S., Kharin, V. V., Lazare, M., Scinocca, J. F., Gillett, N. P., Anstey, J., Arora, V., Christian, J. R., Jiao, Y., Lee, W. G., Majaess, F., Saenko, O. A., Seiler, C., Seinen, C., Shao, A., Solheim, L., von

Salzen, K., Yang, D., Winter, B. and Sigmond, M.: CCCma CanESM5-CanOE model output prepared for CMIP6 ScenarioMIP ssp370, Earth System Grid Federation, , doi:https://doi.org/10.22033/ESGF/CMIP6.10271, 2019d.

Swart, N. C., Cole, J. N. S., Kharin, V. V., Lazare, M., Scinocca, J. F., Gillett, N. P., Anstey, J., Arora, V., Christian, J. R., Jiao, Y., Lee, W. G., Majaess, F., Saenko, O. A., Seiler, C., Seinen, C., Shao, A., Solheim, L., von Salzen, K., Yang, D., Winter, B. and Sigmond, M.: CCCma CanESM5-CanOE model output prepared for CMIP6 ScenarioMIP ssp585, Earth System Grid Federation, , doi:https://doi.org/10.22033/ESGF/CMIP6.10276, 2019e.

Swart, N. C., Cole, J. N. S., Kharin, V. V., Lazare, M., Scinocca, J. F., Gillett, N. P., Anstey, J., Arora, V., Christian, J. R., Jiao, Y., Lee, W. G., Majaess, F., Saenko, O. A., Seiler, C., Seinen, C., Shao, A., Solheim, L., von Salzen, K., Yang, D., Winter, B. and Sigmond, M.: CCCma CanESM5 model output prepared for CMIP6 CMIP abrupt-4xCO2, Earth System Grid Federation, , doi:https://doi.org/10.22033/ESGF/CMIP6.3532, 2019f.

Swart, N. C., Cole, J. N. S., Kharin, V. V., Lazare, M., Scinocca, J. F., Gillett, N. P., Anstey, J., Arora, V. K., Christian, J. R., Jiao, Y., Lee, W. G., Majaess, F., Saenko, O. A., Seiler, C., Seinen, C., Shao, A., Solheim, L., von Salzen, K., Yang, D., Winter, B. and Sigmond, M.: CCCma CanESM5 model output prepared for CMIP6 CMIP historical, Earth System Grid Federation, , doi:https://doi.org/10.22033/ESGF/CMIP6.3610, 2019g.

Swart, N. C., Cole, J. N. S., Kharin, V. V., Lazare, M., Scinocca, J. F., Gillett, N. P., Anstey, J., Arora, V., Christian, J. R., Jiao, Y., Lee, W. G., Majaess, F., Saenko, O. A., Seiler, C., Seinen, C., Shao, A., Solheim, L., von Salzen, K., Yang, D., Winter, B. and Sigmond, M.: CCCma CanESM5 model output prepared for CMIP6 CMIP piControl, Earth System Grid Federation, , doi:https://doi.org/10.22033/ESGF/CMIP6.3673, 2019h.

Swart, N. C., Cole, J. N. S., Kharin, V. V., Lazare, M., Scinocca, J. F., Gillett, N. P., Anstey, J., Arora, V. K., Christian, J. R., Jiao, Y., Lee, W. G., Majaess, F., Saenko, O. A., Seiler, C., Seinen, C., Shao, A., Solheim, L., von Salzen, K., Yang, D., Winter, B. and Sigmond, M.: CCCma CanESM5 model output prepared for CMIP6 ScenarioMIP ssp119, Earth System Grid Federation, , doi:https://doi.org/10.22033/ESGF/CMIP6.3682, 2019i.

Swart, N. C., Cole, J. N. S., Jason, N. ., Kharin, V. V., Lazare, M., Scinocca, J. F., Gillett, N. P., Anstey, J., Arora, V. K., Christian, J. R., Jiao, Y., Lee, W. G., Majaess, F., Saenko, O. A., Seiler, C., Seinen, C., Shao, A., Solheim, L., von Salzen, K., Yang, D., Winter, B. and Sigmond, M.: CCCma CanESM5 model output prepared for CMIP6 ScenarioMIP ssp126, Earth System Grid Federation, , doi:https://doi.org/10.22033/ESGF/CMIP6.3683, 2019j.

Swart, N. C., Cole, J. N. S., Kharin, V. V., Lazare, M., Scinocca, J. F., Gillett, N. P., Anstey, J., Arora, V., Christian, J. R., Jiao, Y., Lee, W. G., Majaess, F., Saenko, O. A., Seiler, C., Seinen, C., Shao, A., Solheim, L., von Salzen, K., Yang, D., Winter, B. and Sigmond, M.: CCCma CanESM5 model output prepared for CMIP6 ScenarioMIP ssp245, Earth System Grid Federation, , doi:https://doi.org/10.22033/ESGF/CMIP6.3685, 2019k.

Swart, N. C., Cole, J. N. S., Kharin, V. V., Lazare, M., Scinocca, J. F., Gillett, N. P., Anstey, J., Arora, V., Christian, J. R., Jiao, Y., Lee, W. G., Majaess, F., Saenko, O. A., Seiler, C., Seinen, C., Shao, A., Solheim, L., von Salzen, K., Yang, D., Winter, B. and Sigmond, M.: CCCma CanESM5 model output prepared for CMIP6 ScenarioMIP ssp370, Earth System Grid Federation, , doi:https://doi.org/10.22033/ESGF/CMIP6.3690, 2019l.

Swart, N. C., Cole, J. N. S., Kharin, V. V., Lazare, M., Scinocca, J. F., Gillett, N. P., Anstey, J., Arora, V., Christian, J. R., Jiao, Y., Lee, W. G., Majaess, F., Saenko, O. A., Seiler, C., Seinen, C., Shao, A., Solheim, L., von Salzen, K., Yang, D., Winter, B. and Sigmond, M.: CCCma CanESM5 model output prepared for CMIP6 ScenarioMIP ssp434, Earth System Grid Federation, , doi:https://doi.org/10.22033/ESGF/CMIP6.3692, 2019m.

Swart, N. C., Cole, J. N. S., Kharin, V. V., Lazare, M., Scinocca, J. F., Gillett, N. P., Anstey, J., Arora, V., Christian, J. R., Jiao, Y., Lee, W. G., Majaess, F., Saenko, O. A., Seiler, C., Seinen, C., Shao, A., Solheim, L., von Salzen, K., Yang, D., Winter, B. and Sigmond, M.: CCCma CanESM5 model output prepared for CMIP6 ScenarioMIP ssp460, Earth System Grid Federation, , doi:https://doi.org/10.22033/ESGF/CMIP6.3693, 2019n.

Swart, N. C., Cole, J. N. S., Kharin, V. V., Lazare, M., Scinocca, J. F., Gillett, N. P., Anstey, J., Arora, V., Christian, J. R., Jiao, Y., Lee, W. G., Majaess, F., Saenko, O. A., Seiler, C., Seinen, C., Shao, A., Solheim, L., von Salzen, K., Yang, D., Winter, B. and Sigmond, M.: CCCma CanESM5 model output prepared for CMIP6 ScenarioMIP ssp585, Earth System Grid Federation, , doi:https://doi.org/10.22033/ESGF/CMIP6.3696, 2019o.

Tachiiri, K., Abe, M., Hajima, T., Arakawa, O., Suzuki, T., Komuro, Y., Ogochi, K., Watanabe, M., Yamamoto, A., Tatebe, H., Noguchi, M. A., Ohgaito, R., Ito, A., Yamazaki, D., Ito, A., Takata, K., Watanabe, S. and Kawamiya, M.: MIROC MIROC-ES2L model output prepared for CMIP6 ScenarioMIP ssp119, Earth System Grid Federation, , doi:https://doi.org/10.22033/ESGF/CMIP6.5740, 2019a.

Tachiiri, K., Abe, M., Hajima, T., Arakawa, O., Suzuki, T., Komuro, Y., Ogochi, K., Watanabe, M., Yamamoto, A., Tatebe, H., Noguchi, M. A., Ohgaito, R., Ito, A., Yamazaki, D., Ito, A., Takata, K., Watanabe, S. and Kawamiya, M.: MIROC MIROC-ES2L model output prepared for CMIP6 ScenarioMIP ssp126, , doi:https://doi.org/10.22033/ESGF/CMIP6.5742, 2019b.

Tachiiri, K., Abe, M., Hajima, T., Arakawa, O., Suzuki, T., Komuro, Y., Ogochi, K., Watanabe, M., Yamamoto, A., Tatebe, H., Noguchi, M. A., Ohgaito, R., Ito, A., Yamazaki, D., Ito, A., Takata, K., Watanabe, S. and Kawamiya, M.: MIROC MIROC-ES2L model output prepared for CMIP6 ScenarioMIP ssp245, Earth System Grid Federation, , doi:https://doi.org/10.22033/ESGF/CMIP6.5745, 2019c.

Tachiiri, K., Abe, M., Hajima, T., Arakawa, O., Suzuki, T., Komuro, Y., Ogochi, K., Watanabe, M., Yamamoto, A., Tatebe, H., Noguchi, M. A., Ohgaito, R., Ito, A., Yamazaki, D., Ito, A., Takata, K., Watanabe, S. and Kawamiya, M.: MIROC MIROC-ES2L model output prepared for CMIP6 ScenarioMIP ssp370, Earth System Grid Federation, , doi:https://doi.org/10.22033/ESGF/CMIP6.5751, 2019d.

Tachiiri, K., Abe, M., Hajima, T., Arakawa, O., Suzuki, T., Komuro, Y., Ogochi, K., Watanabe, M., Yamamoto, A., Tatebe, H., Noguchi, M. A., Ohgaito, R., Ito, A., Yamazaki, D., Ito, A., Takata, K., Watanabe, S. and Kawamiya, M.: MIROC MIROC-ES2L model output prepared for CMIP6 ScenarioMIP ssp585, Earth System Grid Federation, , doi:https://doi.org/10.22033/ESGF/CMIP6.5770, 2019e.

Tang, Y., Rumbold, S., Ellis, R., Kelley, D., Mulcahy, J., Sellar, A., Walton, J. and Jones, C.: MOHC UKESM1.0-LL model output prepared for CMIP6 CMIP abrupt-4xCO2, Earth System Grid Federation, , doi:https://doi.org/10.22033/ESGF/CMIP6.5843, 2019a.

Tang, Y., Rumbold, S., Ellis, R., Kelley, D., Mulcahy, J., Sellar, A., Walton, J. and Jones, C.: MOHC UKESM1.0-LL model output prepared for CMIP6 CMIP piControl, Earth System Grid Federation, , doi:https://doi.org/10.22033/ESGF/CMIP6.6298, 2019b.

Tang, Y., Rumbold, S., Ellis, R., Kelley, D., Mulcahy, J., Sellar, A., Walton, J. and Jones, C.: MOHC UKESM1.0LL model output prepared for CMIP6 CMIP historical, Earth System Grid Federation, , doi:https://doi.org/10.22033/ESGF/CMIP6.6113, 2019c.

Tatebe, H. and Watanabe, M.: MIROC MIROC6 model output prepared for CMIP6 CMIP abrupt-4xCO2, Earth System Grid Federation, , doi:https://doi.org/10.22033/ESGF/CMIP6.5411, 2018a.

Tatebe, H. and Watanabe, M.: MIROC MIROC6 model output prepared for CMIP6 CMIP historical, Earth System

Grid Federation, , doi:https://doi.org/10.22033/ESGF/CMIP6.5603, 2018b.

Tatebe, H. and Watanabe, M.: MIROC MIROC6 model output prepared for CMIP6 CMIP piControl, Earth System Grid Federation, , doi:https://doi.org/10.22033/ESGF/CMIP6.5711, 2018c.

Voldoire, A.: CMIP6 simulations of the CNRM-CERFACS based on CNRM-CM6-1 model for CMIP experiment historical, Earth System Grid Federation, , doi:https://doi.org/10.22033/ESGF/CMIP6.4066, 2018.

Voldoire, A.: CNRM-CERFACS CNRM-CM6-1-HR model output prepared for CMIP6 ScenarioMIP ssp245, Earth System Grid Federation, , doi:https://doi.org/10.22033/ESGF/CMIP6.4190, 2019a.

Voldoire, A.: CNRM-CERFACS CNRM-CM6-1-HR model output prepared for CMIP6 ScenarioMIP ssp585, Earth System Grid Federation, , doi:https://doi.org/10.22033/ESGF/CMIP6.4225, 2019b.

Voldoire, A.: CNRM-CERFACS CNRM-CM6-1 model output prepared for CMIP6 ScenarioMIP for ssp245, Earth System Grid Federation, , doi:https://doi.org/10.22033/ESGF/CMIP6.4189, 2019c.

Voldoire, A.: CNRM-CERFACS CNRM-CM6-1 model output prepared for CMIP6 ScenarioMIP ssp126, Earth System Grid Federation, , doi:https://doi.org/10.22033/ESGF/CMIP6.4184, 2019d.

Voldoire, A.: CNRM-CERFACS CNRM-CM6-1 model output prepared for CMIP6 ScenarioMIP ssp370, Earth System Grid Federation, , doi:https://doi.org/10.22033/ESGF/CMIP6.4197, 2019e.

Voldoire, A.: CNRM-CERFACS CNRM-CM6-1 model output prepared for CMIP6 ScenarioMIP ssp585, Earth System Grid Federation, , doi:https://doi.org/10.22033/ESGF/CMIP6.4224, 2019f.

Voldoire, A.: CNRM-CERFACS CNRM-ESM2-1 model output prepared for CMIP6 ScenarioMIP ssp119, Earth System Grid Federation, , doi:https://doi.org/10.22033/ESGF/CMIP6.4182, 2019g.

Voldoire, A.: CNRM-CERFACS CNRM-ESM2-1 model output prepared for CMIP6 ScenarioMIP ssp126, Earth System Grid Federation, , doi:https://doi.org/10.22033/ESGF/CMIP6.4186, 2019h.

Voldoire, A.: CNRM-CERFACS CNRM-ESM2-1 model output prepared for CMIP6 ScenarioMIP ssp245, Earth System Grid Federation, , doi:https://doi.org/10.22033/ESGF/CMIP6.4191, 2019i.

Voldoire, A.: CNRM-CERFACS CNRM-ESM2-1 model output prepared for CMIP6 ScenarioMIP ssp370, Earth System Grid Federation, , doi:https://doi.org/10.22033/ESGF/CMIP6.4199, 2019j.

Voldoire, A.: CNRM-CERFACS CNRM-ESM2-1 model output prepared for CMIP6 ScenarioMIP ssp434, Earth System Grid Federation, , doi:https://doi.org/10.22033/ESGF/CMIP6.4213, 2019k.

Voldoire, A.: CNRM-CERFACS CNRM-ESM2-1 model output prepared for CMIP6 ScenarioMIP ssp460, Earth System Grid Federation, , doi:https://doi.org/10.22033/ESGF/CMIP6.4217, 2019l.

Voldoire, A.: CNRM-CERFACS CNRM-CM6-1-HR model output prepared for CMIP6 ScenarioMIP ssp126, Earth System Grid Federation, , doi:https://doi.org/10.22033/ESGF/CMIP6.4185, 2020a.

Voldoire, A.: CNRM-CERFACS CNRM-CM6-1-HR model output prepared for CMIP6 ScenarioMIP ssp370, Earth System Grid Federation, , doi:https://doi.org/10.22033/ESGF/CMIP6.4198, 2020b.

Volodin, E., Mortikov, E., Gritsun, A., Lykossov, V., Galin, V., Diansky, N., Gusev, A., Kostrykin, S., Iakovlev, N., Shestakova, A. and Emelina, S.: INM INM-CM4-8 model output prepared for CMIP6 CMIP abrupt-4xCO2, Earth System Grid Federation, , doi:https://doi.org/10.22033/ESGF/CMIP6.4931, 2019a.

Volodin, E., Mortikov, E., Gritsun, A., Lykossov, V., Galin, V., Diansky, N., Gusev, A., Kostrykin, S., Iakovlev, N., Shestakova, A. and Emelina, S.: INM INM-CM4-8 model output prepared for CMIP6 CMIP historical, Earth

System Grid Federation, , doi:https://doi.org/10.22033/ESGF/CMIP6.5069, 2019b.

Volodin, E., Mortikov, E., Gritsun, A., Lykossov, V., Galin, V., Diansky, N., Gusev, A., Kostrykin, S., Iakovlev, N., Shestakova, A. and Emelina, S.: INM INM-CM4-8 model output prepared for CMIP6 CMIP piControl, Earth System Grid Federation, , doi:https://doi.org/10.22033/ESGF/CMIP6.5080, 2019c.

Volodin, E., Mortikov, E., Gritsun, A., Lykossov, V., Galin, V., Diansky, N., Gusev, A., Kostrykin, S., Iakovlev, N., Shestakova, A. and Emelina, S.: INM INM-CM4-8 model output prepared for CMIP6 ScenarioMIP ssp126, Earth System Grid Federation, , doi:https://doi.org/10.22033/ESGF/CMIP6.12325, 2019d.

Volodin, E., Mortikov, E., Gritsun, A., Lykossov, V., Galin, V., Diansky, N., Gusev, A., Kostrykin, S., Iakovlev, N., Shestakova, A. and Emelina, S.: INM INM-CM4-8 model output prepared for CMIP6 ScenarioMIP ssp245, Earth System Grid Federation, , doi:https://doi.org/10.22033/ESGF/CMIP6.12327, 2019e.

Volodin, E., Mortikov, E., Gritsun, A., Lykossov, V., Galin, V., Diansky, N., Gusev, A., Kostrykin, S., Iakovlev, N., Shestakova, A. and Emelina, S.: INM INM-CM4-8 model output prepared for CMIP6 ScenarioMIP ssp370, Earth System Grid Federation, , doi:https://doi.org/10.22033/ESGF/CMIP6.12329, 2019f.

Volodin, E., Mortikov, E., Gritsun, A., Lykossov, V., Galin, V., Diansky, N., Gusev, A., Kostrykin, S., Iakovlev, N., Shestakova, A. and Emelina, S.: INM INM-CM4-8 model output prepared for CMIP6 ScenarioMIP ssp585, Earth System Grid Federation, , doi:https://doi.org/10.22033/ESGF/CMIP6.12337, 2019g.

Volodin, E., Mortikov, E., Gritsun, A., Lykossov, V., Galin, V., Diansky, N., Gusev, A., Kostrykin, S., Iakovlev, N., Shestakova, A. and Emelina, S.: INM INM-CM5-0 model output prepared for CMIP6 CMIP historical, Earth System Grid Federation, , doi:https://doi.org/10.22033/ESGF/CMIP6.5070, 2019h.

Volodin, E., Mortikov, E., Gritsun, A., Lykossov, V., Galin, V., Diansky, N., Gusev, A., Kostrykin, S., Iakovlev, N., Shestakova, A. and Emelina, S.: INM INM-CM5-0 model output prepared for CMIP6 ScenarioMIP ssp126, Earth System Grid Federation, , doi:https://doi.org/10.22033/ESGF/CMIP6.12326, 2019i.

Volodin, E., Mortikov, E., Gritsun, A., Lykossov, V., Galin, V., Diansky, N., Gusev, A., Kostrykin, S., Iakovlev, N., Shestakova, A. and Emelina, S.: INM INM-CM5-0 model output prepared for CMIP6 ScenarioMIP ssp245, Earth System Grid Federation, , doi:https://doi.org/10.22033/ESGF/CMIP6.12328, 2019j.

Volodin, E., Mortikov, E., Gritsun, A., Lykossov, V., Galin, V., Diansky, N., Gusev, A., Kostrykin, S., Iakovlev, N., Shestakova, A. and Emelina, S.: INM INM-CM5-0 model output prepared for CMIP6 ScenarioMIP ssp370, Earth System Grid Federation, , doi:https://doi.org/10.22033/ESGF/CMIP6.12330, 2019k.

Volodin, E., Mortikov, E., Gritsun, A., Lykossov, V., Galin, V., Diansky, N., Gusev, A., Kostrykin, S., Iakovlev, N., Shestakova, A. and Emelina, S.: INM INM-CM5-0 model output prepared for CMIP6 ScenarioMIP ssp585, Earth System Grid Federation, , doi:https://doi.org/10.22033/ESGF/CMIP6.12338, 2019l.

Volodin, E., Mortikov, E., Gritsun, A., Lykossov, V., Galin, V., Diansky, N., Gusev, A., Kostrykin, S., Iakovlev, N., Shestakova, A. and Emelina, S.: NM INM-CM5-0 model output prepared for CMIP6 CMIP abrupt-4xCO2, Earth System Grid Federation, , doi:https://doi.org/10.22033/ESGF/CMIP6.4932, 2019m.

Volodin, E., Mortikov, E., Gritsun, A., Lykossov, V., Galin, V., Diansky, N., Gusev, A., Kostrykin, S., Iakovlev, N., Shestakova, A. and Emelina, S.: NM INM-CM5-0 model output prepared for CMIP6 CMIP piControl, Earth System Grid Federation, , doi:https://doi.org/10.22033/ESGF/CMIP6.5081, 2019n.

Wieners, K.-H., Giorgetta, M., Jungclaus, J. H., Reick, C., Esch, M., Bittner, M., Legutke, S., Schupfner, M., Wachsmann, F., Gayler, V., Haak, H., de Vrese, P., Raddatz, T., Mauritsen, T., von Storch, J.-S., Behrens, J., Brovkin, V., Claussen, M., Crueger, T., Fast, I., Fiedler, S., Hagemann, S., Hohenegger, C., Jahns, T., Kloster, S., Kinne, S., Lasslop, G., Kornblueh, L., Marotzke, J., Matei, D., Meraner, K., Mikolajewicz, U., Modali, K., Muller, W., Nabel, J. E. M. S., Notz, D., Peters, K., Pincus, R., Pohlmann, H., Pongratz, J., Rast, S., Schmidt, H., Schnur, R., Schulzweida, U., Six, K., Stevens, B., Voigt, A. and Roeckner, E.: MPI-M MPI-ESM1.2-LR model output prepared for CMIP6 CMIP historical, Earth System Grid Federation, , doi:https://doi.org/10.22033/ESGF/CMIP6.6595, 2019a.

Wieners, K.-H., Giorgetta, M., Jungclaus, J., Reick, C., Esch, M., Bittner, M., Gayler, V., Haak, H., de Vrese, P., Raddatz, T., Mauritsen, T., von Storch, J.-S., Behrens, J., Brovkin, V., Claussen, M., Crueger, T., Fast, I., Fiedler, S., Hagemann, S., Hohenegger, C., Jahns, T., Kloster, S., Kinne, S., Lasslop, G., Kornblueh, L., Marotzke, J., Matei, D., Meraner, K., Mikolajewicz, U., Modali, K., Müller, W., Nabel, J., Notz, D., Peters, K., Pincus, R., Pohlmann, H., Pongratz, J., Rast, S., Schmidt, H., Schnur, R., Schulzweida, U., Six, K., Stevens, B., Voigt, A. and Roeckner, E.: MPI-M MPI-ESM1.2-LR model output prepared for CMIP6 ScenarioMIP ssp126, Earth System Grid Federation, , doi:https://doi.org/10.22033/ESGF/CMIP6.6690, 2019b.

Wieners, K.-H., Giorgetta, M., Jungclaus, J., Reick, C., Esch, M., Bittner, M., Gayler, V., Haak, H., de Vrese, P., Raddatz, T., Mauritsen, T., von Storch, J.-S., Behrens, J., Brovkin, V., Claussen, M., Crueger, T., Fast, I., Fiedler, S., Hagemann, S., Hohenegger, C., Jahns, T., Kloster, S., Kinne, S., Lasslop, G., Kornblueh, L., Marotzke, J., Matei, D., Meraner, K., Mikolajewicz, U., Modali, K., Müller, W., Nabel, J., Notz, D., Peters, K., Pincus, R., Pohlmann, H., Pongratz, J., Rast, S., Schmidt, H., Schnur, R., Schulzweida, U., Six, K., Stevens, B., Voigt, A. and Roeckner, E.: MPI-M MPI-ESM1.2-LR model output prepared for CMIP6 ScenarioMIP ssp245, Earth System Grid Federation, , doi:https://doi.org/10.22033/ESGF/CMIP6.6693, 2019c.

Wieners, K.-H., Giorgetta, M., Jungclaus, J., Reick, C., Esch, M., Bittner, M., Gayler, V., Haak, H., de Vrese, P., Raddatz, T., Mauritsen, T., von Storch, J.-S., Behrens, J., Brovkin, V., Claussen, M., Crueger, T., Fast, I., Fiedler, S., Hagemann, S., Hohenegger, C., Jahns, T., Kloster, S., Kinne, S., Lasslop, G., Kornblueh, L., Marotzke, J., Matei, D., Meraner, K., Mikolajewicz, U., Modali, K., Müller, W., Nabel, J., Notz, D., Peters, K., Pincus, R., Pohlmann, H., Pongratz, J., Rast, S., Schmidt, H., Schnur, R., Schulzweida, U., Six, K., Stevens, B., Voigt, A. and Roeckner, E.: MPI-M MPI-ESM1.2-LR model output prepared for CMIP6 ScenarioMIP ssp370, Earth System Grid Federation, , doi:https://doi.org/10.22033/ESGF/CMIP6.6695, 2019d.

Wieners, K.-H., Giorgetta, M., Jungclaus, J., Reick, C., Esch, M., Bittner, M., Gayler, V., Haak, H., de Vrese, P., Raddatz, T., Mauritsen, T., von Storch, J.-S., Behrens, J., Brovkin, V., Claussen, M., Crueger, T., Fast, I., Fiedler, S., Hagemann, S., Hohenegger, C., Jahns, T., Kloster, S., Kinne, S., Lasslop, G., Kornblueh, L., Marotzke, J., Matei, D., Meraner, K., Mikolajewicz, U., Modali, K., Müller, W., Nabel, J., Notz, D., Peters, K., Pincus, R., Pohlmann, H., Pongratz, J., Rast, S., Schmidt, H., Schnur, R., Schulzweida, U., Six, K., Stevens, B., Voigt, A. and Roeckner, E.: MPI-M MPI-ESM1.2-LR model output prepared for CMIP6 ScenarioMIP ssp585, Earth System Grid Federation, , doi:https://doi.org/10.22033/ESGF/CMIP6.6705, 2019e.

Wu, T., Chu, M., Dong, M., Fang, Y., Jie, W., Li, J., Li, W., Liu, Q., Shi, X., Xin, X., Yan, J., Zhang, F., Zhang, J., Zhang, L. and Zhang, Y.: BCC BCC-CSM2MR model output prepared for CMIP6 CMIP abrupt-4xCO2, Earth System Grid Federation, , doi:https://doi.org/10.22033/ESGF/CMIP6.2845, 2018a.

Wu, T., Chu, M., Dong, M., Fang, Y., Jie, W., Li, J., Li, W., Liu, Q., Shi, X., Xin, X., Yan, J., Zhang, F., Zhang, J., Zhang, L. and Zhang, Y.: BCC BCC-CSM2MR model output prepared for CMIP6 CMIP historical, Earth System Grid Federation, , doi:https://doi.org/10.22033/ESGF/CMIP6.2948, 2018b.

Wu, T., Chu, M., Dong, M., Fang, Y., Jie, W., Li, J., Li, W., Liu, Q., Shi, X., Xin, X., Yan, J., Zhang, F., Zhang, J., Zhang, L. and Zhang, Y.: BCC BCC-CSM2MR model output prepared for CMIP6 CMIP piControl, Earth System Grid Federation, , doi:https://doi.org/10.22033/ESGF/CMIP6.3016, 2018c.

Xin, X., Wu, T., Shi, X., Zhang, F., Li, J., Chu, M., Liu, Q., Yan, J., Ma, Q. and Wei, M.: BCC BCC-CSM2MR model output prepared for CMIP6 ScenarioMIP ssp126, Earth System Grid Federation, , doi:https://doi.org/10.22033/ESGF/CMIP6.3028, 2019a.

Xin, X., Wu, T., Shi, X., Zhang, F., Li, J., Chu, M., Liu, Q., Yan, J., Ma, Q. and Wei, M.: BCC BCC-CSM2MR model output prepared for CMIP6 ScenarioMIP ssp245, Earth System Grid Federation, , doi:https://doi.org/10.22033/ESGF/CMIP6.3030, 2019b.

Xin, X., Wu, T., Shi, X., Zhang, F., Li, J., Chu, M., Liu, Q., Yan, J., Ma, Q. and Wei, M.: BCC BCC-CSM2MR model output prepared for CMIP6 ScenarioMIP ssp370, Earth System Grid Federation, , doi:https://doi.org/10.22033/ESGF/CMIP6.3035, 2019c.

Xin, X., Wu, T., Shi, X., Zhang, F., Li, J., Chu, M., Liu, Q., Yan, J., Ma, Q. and Wei, M.: BCC BCC-CSM2MR model output prepared for CMIP6 ScenarioMIP ssp585, Earth System Grid Federation, , doi:https://doi.org/10.22033/ESGF/CMIP6.3050, 2019d.

YU, Y.: CAS FGOALS-f3-L model output prepared for CMIP6 CMIP historical, Earth System Grid Federation, , doi:https://doi.org/10.22033/ESGF/CMIP6.3355, 2019a.

YU, Y.: CAS FGOALS-f3-L model output prepared for CMIP6 ScenarioMIP ssp126, Earth System Grid Federation, , doi:https://doi.org/10.22033/ESGF/CMIP6.3464, 2019b.

YU, Y.: CAS FGOALS-f3-L model output prepared for CMIP6 ScenarioMIP ssp245, Earth System Grid Federation, , doi:https://doi.org/10.22033/ESGF/CMIP6.3468, 2019c.

YU, Y.: CAS FGOALS-f3-L model output prepared for CMIP6 ScenarioMIP ssp370, Earth System Grid Federation, , doi:https://doi.org/10.22033/ESGF/CMIP6.3479, 2019d.

YU, Y.: CAS FGOALS-f3-L model output prepared for CMIP6 ScenarioMIP ssp585, Earth System Grid Federation, , doi:https://doi.org/10.22033/ESGF/CMIP6.3502, 2019e.

Yukimoto, S., Koshiro, T., Kawai, H., Oshima, N., Yoshida, K., Urakawa, S., Tsujino, H., Deushi, M., Tanaka, T., Hosaka, M., Yoshimura, H., Shindo, E., Mizuta, R., Ishii, M., Obata, A. and Adachi, Y.: MRI MRI-ESM2.0 model output prepared for CMIP6 CMIP historical, Earth System Grid Federation, , doi:https://doi.org/10.22033/ESGF/CMIP6.6842, 2019a.

Yukimoto, S., Koshiro, T., Kawai, H., Oshima, N., Yoshida, K., Urakawa, S., Tsujino, H., Deushi, M., Tanaka, T., Hosaka, M., Yoshimura, H., Shindo, E., Mizuta, R., Ishii, M., Obata, A. and Adachi, Y.: MRI MRI-ESM2.0 model output prepared for CMIP6 ScenarioMIP ssp119, Earth System Grid Federation, , doi:https://doi.org/10.22033/ESGF/CMIP6.6908, 2019b.

Yukimoto, S., Koshiro, T., Kawai, H., Oshima, N., Yoshida, K., Urakawa, S., Tsujino, H., Deushi, M., Tanaka, T., Hosaka, M., Yoshimura, H., Shindo, E., Mizuta, R., Ishii, M., Obata, A. and Adachi, Y.: MRI MRI-ESM2.0 model output prepared for CMIP6 ScenarioMIP ssp126, Earth System Grid Federation, , doi:https://doi.org/10.22033/ESGF/CMIP6.6909, 2019c.

Yukimoto, S., Koshiro, T., Kawai, H., Oshima, N., Yoshida, K., Urakawa, S., Tsujino, H., Deushi, M., Tanaka, T., Hosaka, M., Yoshimura, H., Shindo, E., Mizuta, R., Ishii, M., Obata, A. and Adachi, Y.: MRI MRI-ESM2.0 model output prepared for CMIP6 ScenarioMIP ssp245, Earth System Grid Federation, , doi:https://doi.org/10.22033/ESGF/CMIP6.6910, 2019d.

Yukimoto, S., Koshiro, T., Kawai, H., Oshima, N., Yoshida, K., Urakawa, S., Tsujino, H., Deushi, M., Tanaka, T., Hosaka, M., Yoshimura, H., Shindo, E., Mizuta, R., Ishii, M., Obata, A. and Adachi, Y.: MRI MRI-ESM2.0 model output prepared for CMIP6 ScenarioMIP ssp370, Earth System Grid Federation, , doi:https://doi.org/10.22033/ESGF/CMIP6.6915, 2019e.

Yukimoto, S., Koshiro, T., Kawai, H., Oshima, N., Yoshida, K., Urakawa, S., Tsujino, H., Deushi, M., Tanaka, T., Hosaka, M., Yoshimura, H., Shindo, E., Mizuta, R., Ishii, M., Obata, A. and Adachi, Y.: MRI MRI-ESM2.0 model output prepared for CMIP6 ScenarioMIP ssp434, Earth System Grid Federation, , doi:https://doi.org/10.22033/ESGF/CMIP6.6925, 2019f.

Yukimoto, S., Koshiro, T., Kawai, H., Oshima, N., Yoshida, K., Urakawa, S., Tsujino, H., Deushi, M., Tanaka, T., Hosaka, M., Yoshimura, H., Shindo, E., Mizuta, R., Ishii, M., Obata, A. and Adachi, Y.: MRI MRI-ESM2.0 model output prepared for CMIP6 ScenarioMIP ssp460, Earth System Grid Federation, , doi:https://doi.org/10.22033/ESGF/CMIP6.6926, 2019g.

Yukimoto, S., Koshiro, T., Kawai, H., Oshima, N., Yoshida, K., Urakawa, S., Tsujino, H., Deushi, M., Tanaka, T., Hosaka, M., Yoshimura, H., Shindo, E., Mizuta, R., Ishii, M., Obata, A. and Adachi, Y.: MRI MRI-ESM2.0 model output prepared for CMIP6 ScenarioMIP ssp585, Earth System Grid Federation, , doi:https://doi.org/10.22033/ESGF/CMIP6.6929, 2019h.

Zhang, J., Wu, T., Shi, X., Zhang, F., Li, J., Chu, M., Liu, Q., Yan, J., Ma, Q. and Wei, M.: BCC BCC-ESM1 model output prepared for CMIP6 CMIP historical, Earth System Grid Federation, , doi:https://doi.org/10.22033/ESGF/CMIP6.2949, 2018a.

Zhang, J., Wu, T., Shi, X., Zhang, F., Li, J., Chu, M., Liu, Q., Yan, J., Ma, Q. and Wei, M.: BCC BCC-ESM1 model output prepared for CMIP6 CMIP piControl, Earth System Grid Federation, , doi:https://doi.org/10.22033/ESGF/CMIP6.3017, 2018b.

Zhang, J., Wu, T., Shi, X., Zhang, F., Li, J., Chu, M., Liu, Q., Yan, J., Ma, Q. and Wei, M.: BCC BCC-ESM1 model output prepared for CMIP6 CMIP abrupt-4xCO2, Earth System Grid Federation, , doi:https://doi.org/10.22033/ESGF/CMIP6.2846, 2019.

Ziehn, T., Chamberlain, M., Lenton, A., Law, R., Bodman, R., Dix, M., Wang, Y., Dobrohotoff, P., Srbinovsky, J., Stevens, L., Vohralik, P., Mackallah, C., Sullivan, A., O’Farrell, S. and Druken, K.: CSIRO ACCESS-ESM1.5 model output prepared for CMIP6 CMIP abrupt-4xCO2, Earth System Grid Federation, , doi:https://doi.org/10.22033/ESGF/CMIP6.4238, 2019a.

Ziehn, T., Chamberlain, M., Lenton, A., Law, R., Bodman, R., Dix, M., Wang, Y., Dobrohotoff, P., Srbinovsky, J., Stevens, L., Vohralik, P., Mackallah, C., Sullivan, A., O’Farrell, S. and Druken, K.: CSIRO ACCESS-ESM1.5 model output prepared for CMIP6 CMIP historical, Earth System Grid Federation, , doi:https://doi.org/10.22033/ESGF/CMIP6.4272, 2019b.

Ziehn, T., Chamberlain, M., Lenton, A., Law, R., Bodman, R., Dix, M., Wang, Y., Dobrohotoff, P., Srbinovsky, J., Stevens, L., Vohralik, P., Mackallah, C., Sullivan, A., O’Farrell, S. and Druken, K.: CSIRO ACCESS-ESM1.5 model output prepared for CMIP6 CMIP piControl, Earth System Grid Federation, , doi:https://doi.org/10.22033/ESGF/CMIP6.4312, 2019c.

Ziehn, T., Chamberlain, M., Lenton, A., Law, R., Bodman, R., Dix, M., Wang, Y., Dobrohotoff, P., Srbinovsky, J., Stevens, L., Vohralik, P., Mackallah, C., Sullivan, A., O’Farrell, S. and Druken, K.: CSIRO ACCESS-ESM1.5 model output prepared for CMIP6 ScenarioMIP ssp126, Earth System Grid Federation, , doi:https://doi.org/10.22033/ESGF/CMIP6.4320, 2019d.

Ziehn, T., Chamberlain, M., Lenton, A., Law, R., Bodman, R., Dix, M., Wang, Y., Dobrohotoff, P., Srbinovsky, J., Stevens, L., Vohralik, P., Mackallah, C., Sullivan, A., O’Farrell, S. and Druken, K.: CSIRO ACCESS-ESM1.5 model output prepared for CMIP6 ScenarioMIP ssp245, Earth System Grid Federation, , doi:https://doi.org/10.22033/ESGF/CMIP6.4322, 2019e.

Ziehn, T., Chamberlain, M., Lenton, A., Law, R., Bodman, R., Dix, M., Wang, Y., Dobrohotoff, P., Srbinovsky, J., Stevens, L., Vohralik, P., Mackallah, C., Sullivan, A., O’Farrell, S. and Druken, K.: CSIRO ACCESS-ESM1.5 model output prepared for CMIP6 ScenarioMIP ssp370, Earth System Grid Federation, , doi:https://doi.org/10.22033/ESGF/CMIP6.4324, 2019f.

Ziehn, T., Chamberlain, M., Lenton, A., Law, R., Bodman, R., Dix, M., Wang, Y., Dobrohotoff, P., Srbinovsky, J., Stevens, L., Vohralik, P., Mackallah, C., Sullivan, A., O’Farrell, S. and Druken, K.: CSIRO ACCESS-ESM1.5 model output prepared for CMIP6 ScenarioMIP ssp585, Earth System Grid Federation, , doi:https://doi.org/10.22033/ESGF/CMIP6.4333, 2019g.